International Journal of Scientific Research and Engineering Development-– Volume 6 Issue 4, July- Aug 2023

Available at www.ijsred.com

RESEARCH ARTICLE OPEN ACCESS

Petrophysical Evaluation of Reservoirs in Gabo Field, Onshore Niger Delta, Nigeria

Belema F. Jamabo[1], Godwin J. Udom[2] and Godwin O. Emujakporue[3]

[1](World Bank Centre of Excellence for Oil Field Research, University of Port Harcourt, Port Harcourt.
Email: belemaj@gmail.com)

[2](Department of Geology, University of Port Harcourt, Port Harcourt.
Email: godwin.udom@uniport.edu.ng)

[3](Department of Physics, University of Port Harcourt, Port Harcourt.
Email: owin20009@yahoo.com)

Abstract

The evaluation of petrophysical characteristics of reservoirs in Gabo field was carried out using geophysical wireline logs provided for six (6) wells. The main petrophysical parameters evaluated were Volume of shale, permeability, porosity, hydrocarbon saturation and water saturation. A total of four (4)reservoirs wereidentified (reservoir A, B, C and D). The reservoir sands exhibit porosity values ranging from 9% -26%, while the estimated permeability values lie between 734mD and 1209mD. The Porosity values are considered to be good to very good whereas the permeability values range from very good to excellent. Several sub environments were recognised based on GR log shapes. They include: Fluvial channels, Delta front, shore face, tidal flat environment. The overall depositional environment has been inferred to be most likely within the Coastal deltaic- Outer Neritic depositional environment.

Keywords- **Hydrocarbon, Reservoir, Petrophysical evaluation , Porosity and Permeability**

I. INTRODUCTION

Petrophysics is the study of the physical and chemical properties of rocks and their contained fluids. It is the foundation upon which formation evaluation and reservoir analysis are built. Petrophysical properties of the rocks largely depend on theconditions of the environment of deposition that controlled the mineral composition, grain size, orientation or packing, amount of cementation and packing. A major application of petrophysics is in studying reservoirs for the hydrocarbon industry. Petrophysical analysis are employed to help reservoir engineers and geoscientists understand the rock properties of the reservoir, particularly how pores in the subsurface are interconnected, controlling the accumulation and migration of hydrocarbons. It can also be used to study the lateral change in content of fluids as it helps presume the lateral continuity or extent of the reservoir when seismic data is not available [1].In addition, studying the spatial uniformity of the saturating reservoir fluids can be crucial to oil and gas production. This further mitigates failure in hydrocarbon exploration.

A good analysis of modern suite of logs can infer the thickness, porosity, water saturation, hydrocarbon type and saturation, mechanical properties, lithology and environment of deposition, pore pressure, dip and bedding features. Therefore, estimates of lithology, fluid content and porosity are indispensable. A key aspect of petrophysics is measuring and evaluating these rock properties by acquiring well log measurements, core measurements, and seismic measurements. These studies are then combined with geological, geophysical and reservoir engineeringstudies to give a complete picture of the reservoir.Most reservoir hydrocarbons reside in the microscopic pore spaces or open fractures of sedimentary rocks like sandstones.To produce them, detailed petrophysical and sequence stratigraphy knowledge are needed to guide the placement of production platforms and well paths [2]. This can consequently help to optimize hydrocarbon recovery, and to improve predictions of reservoir performance.

Petroleum geologists must have a good knowledge of petrophysicsin order to find oil reservoirs and devise the best plan of getting it out of the ground before drilling can begin.

In this study the objectives using the geophysical wireline logs include: determination of the depositional environment, estimate and compare the porosity, permeability, water saturation and hydrocarbon saturation across the identified reservoirs and predict the reservoir quality.

II. STUDY AREA

Gabo field is an onshore Nigeria oil field. The study area (Fig 1) is located between Latitude 4^0 31' E – 4^0 35' E and Longitude 5^0 25' N – 5^0 26' N, consisting of six (6) wells designate Gabo-4, Gabo-12, Gabo-13, Gabo-20, Gabo 30 and Gabo-57 (Fig 2).

Fig 1: Map Showing the location of Gabo Field in the Central Swamp Depobelt, Niger Delta.

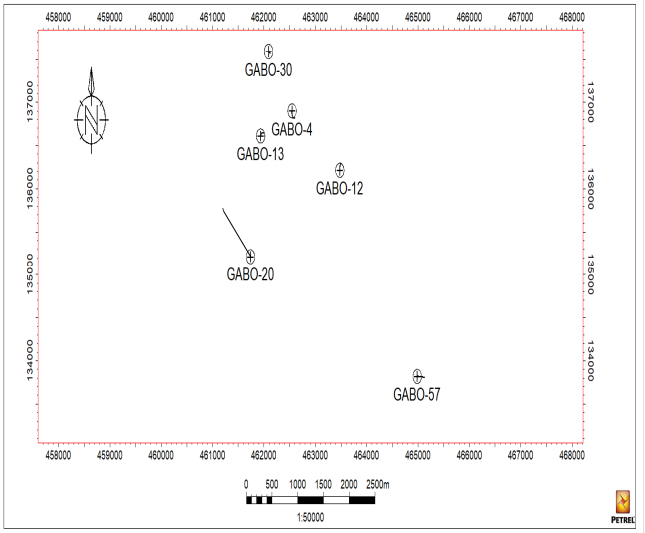

Fig 2: Base Map of the location

III. MATERIALS AND METHODS

The data set for this research was provided by Total Exploration and Production Nigeria limited (Total E &P) through the approval from the Department of Petroleum Resources (DPR), Nigeria.

The suite of well logs provided for this research comprises of gamma ray (GR), spontaneous potential (SP), gamma ray index, resistivity and density logs. The software used for the analysis were Schlumberger petrel (2014 version) and Microsoft excel.

A. Research Workflow

The research design used for this study is shown in Fig 3. Various analysis and interpretations were applied to the well logs data used for the study.

.

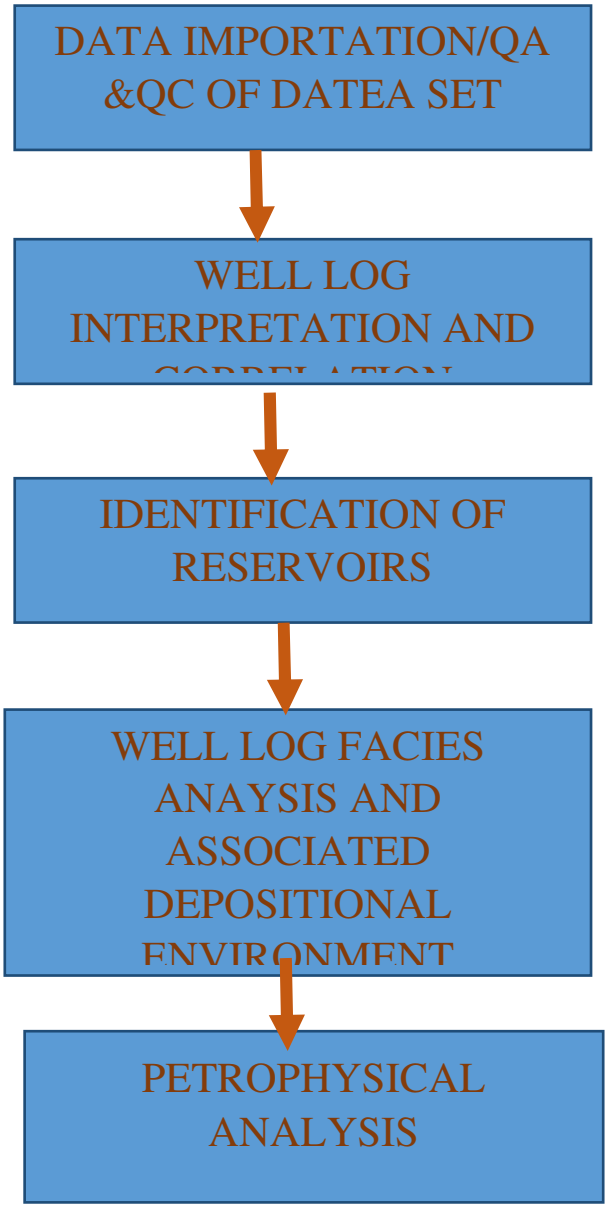

Fig 3: Showing the research workflow

B. Data Importation/ Quality control of data set

The wireline data used in this research was imported into Petrel software. The geographical location of the field was first imputed, followed by the well header which was matched with the appropriate file type. The various logs were imported and were matched with the various well heads before the well deviation data were imported. The quality control was applied to the well headers, well deviation data and the well logs.

C. Stratigraphic Correlations of Reservoir Sands

Detailed correlation of Gabo field was carried out using six (6) wells with the aid of relevant normalized petrophysical logs and other parameters.The correlation of the horizons was carried out with the reservoir tops and bottoms. In attempting to carry out a stratigraphic correlation across wells, one has to understand the regional settings of the hydrocarbon field through field base maps or by developing a cross section along wells; this will enhance a better stratigraphic correlation. Reference [3] also suggested the importance of having cross sections for the entire field in performing stratigraphic correlation of reservoir sands across the field as this will reveal a regional section of the exploration field as well as the sequence in which these formations were deposited. However, it is worth mentioning that Stratigraphic correlation can be however carried out effectively with well logs cross sections in the absence of seismic sections.

D. Identification of Reservoirs

In the sand units delineated, differentiation between reservoir fluids (hydrocarbon and water) was done using the resistivity log. Since the resistivity of hydrocarbon is higher than that of the formation water [4], hydrocarbon sand unitswere inferred from high resistivity values observed from the deep resistivity reading.

Based on the Log motif characteristics, top and bottom horizons were selected to mark each identified reservoir, and then correlation was carried out across wells using this identified log motif to understand the stratigraphy of the reservoir sands which includes both lateral continuity as well as termination of reservoir sands across the field.

E. Evaluation of Reservoir Petrophysical Properties

Petrophysical properties were calculated and estimated for the different identified hydrocarbon bearing reservoirs.

1. Determination of volume of shale (V_{SH})

The volume of shale is best determined from the gamma ray log. The presence of shale in the reservoir makes porosity logs to record high porosity, lower water saturation values and causes low resistivity readings.

Gamma ray index (IGR)

$$I_{GR} = \frac{GR_{log} - GR_{min}}{GR_{max} - GR_{min}}$$

Equation after reference [5],

Where;

I_{GR} = *Gamma ray index that describes a linear response to shale content*

GR_{log} = *Log reading at depth interest*

GR_{min} = *Gamma ray value in a nearby clean sand zone*

GR_{max} = *Gamma ray value in a nearby shale.*

Volume Shale (V_{SH})

$$V_{SH} = 0.083 * \left(2^{(3.7 * GR_{index})} - 1\right) \quad \text{....2}$$

Equation after reference [6] of non-linear relationship for Tertiary rocks, where;

V_{SH} = *Volume of shale*

I_{GR} = *Gamma ray index that describes a linear response to shale content*

2. Determination of Total Porosity (POROT)

$$\emptyset_T = \frac{\rho_{ma} - \rho_{bulk}}{\rho_{ma} - \rho_{fl}} \quad \text{....3}$$

Where;

$\emptyset_T$ = *Total porosity*

ρ_{ma}= *Matrix density = 2.65*

ρ_{bulk}= *Bulk density*

ρ_{fl} = *Fluid density (0.74 for gas, 0.9 for oil and 1.0 for water)*

3. Effective Porosity (POROE)

$$\emptyset_e = \emptyset_T - (\emptyset t_{sh} \times V_{SH}) \quad \text{.....4}$$

Where;

$\emptyset_e$ = *Effective porosity*

$\emptyset t_{sh}$ = *Total shale porosity*

$\emptyset_T$ = *Total porosity*

V_{SH} = *Volume of shale*

4. Determination of Water Saturation (Sw)

This is the water saturation of the invaded zone. It is the percentage of pore volume in a rock which is occupied by formation water; it is expressed as percentage or fraction. Water saturation is an important factor in reservoir evaluation because hydrocarbon can be estimated from it.

$$S_w = \sqrt{\frac{R_o}{R_t}} \quad \text{....5}$$

Where;

S_w= *Water saturation*

R_o = *Resistivity of the oil leg*

R_t = *True resistivity reading*

5. Determination of Hydrocarbon Saturation (S_H)

Hydrocarbon saturation is the percentage or fraction of pore volume occupied by hydrocarbon. It is usually determined by the difference between unity and water saturation in fraction. It is given by:

$$S_H = 1 - S_w \quad \text{.....6}$$

Where;

S_H = *Hydrocarbon saturation*

S_w= *Water saturation*

6. Determination of Permeability (K)

Permeability is the measure of the ease with which a formation permits a fluid to flow through it. To be permeable a rock must have interconnected pore spaces.

$$K(mD) = 307 + 26552(\emptyset_e^2) - 34540\ (\emptyset_e \times S_w)^2 \quad \text{....7}$$

Equation after reference [7], where;

K(mD) = Permeability in milliDarcy

$\emptyset_e$ = *Effective porosity*

S_w= *Water saturation*

IV. RESULTS AND DISCUSSIONS

A. Field-Wide Horizon and Datum Correlation

A correlation plan was established where major correlation profiles were taken along the strike direction that is the North west–South east direction (Fig 4). The generated well correlated panels along the strike direction are shown in (Fig 5a-5e) respectively. This offered the opportunity to analyse the architectural, structural and stratigraphic elements and their play concepts across the entire block. This was achieved using stratigraphic tops, reservoir tops and bottoms.

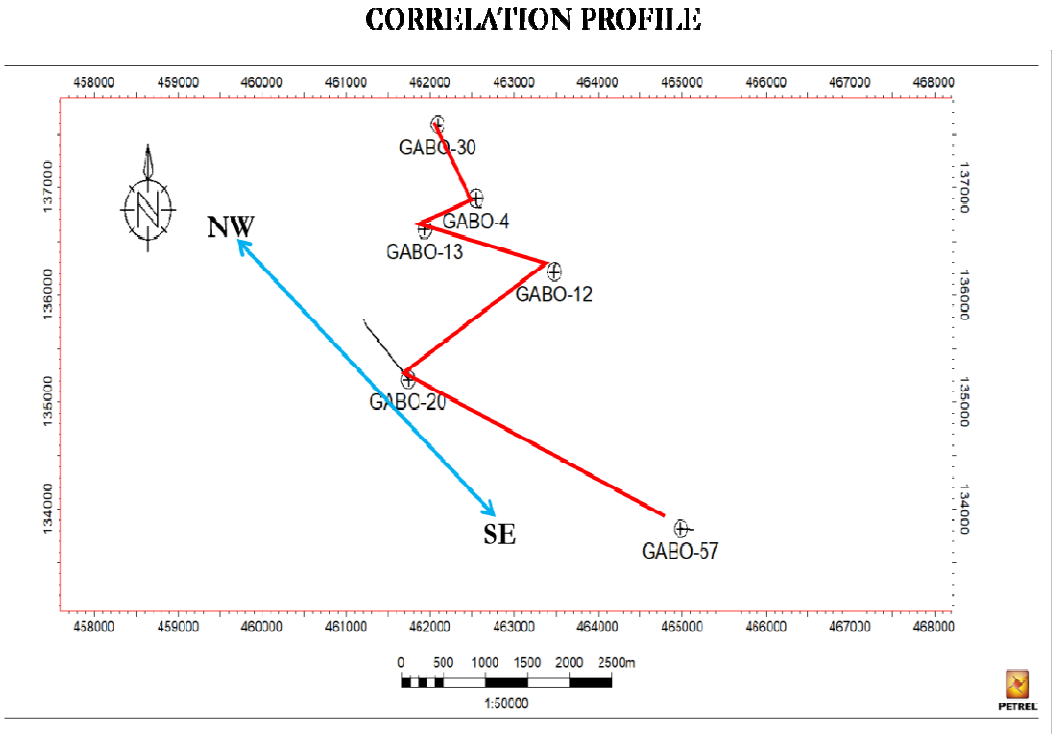

Fig 4. Correlation Profile

NW **SE**

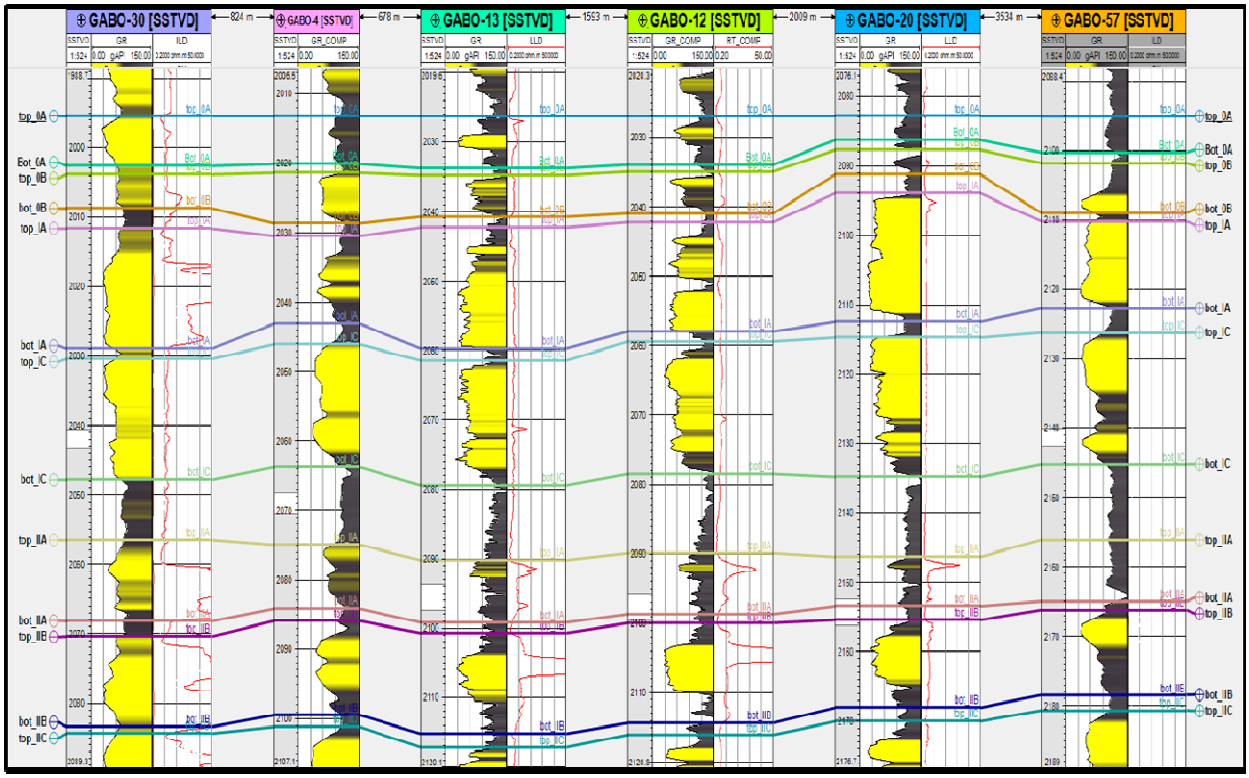

Fig 5a. Gabo well correlation along strike direction 1/5

NW **SE**

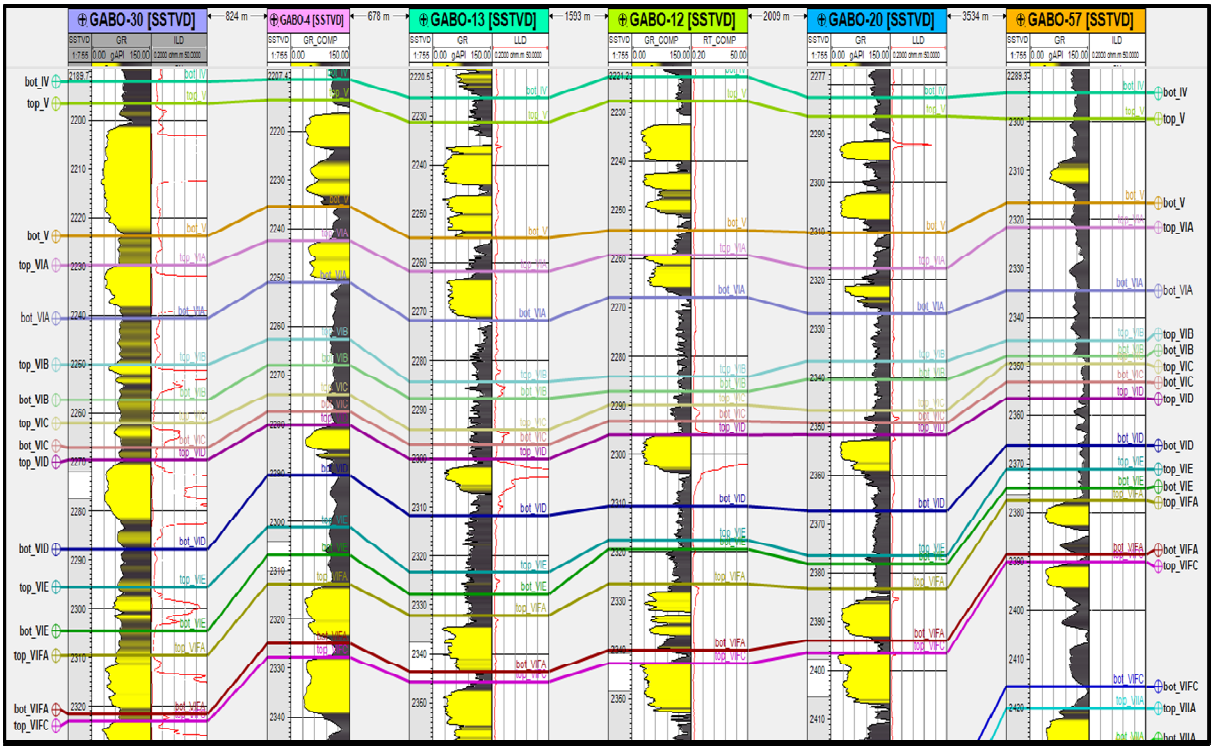

Figure 5b: Gabo well correlation along strike direction 2/5

NW **SE**

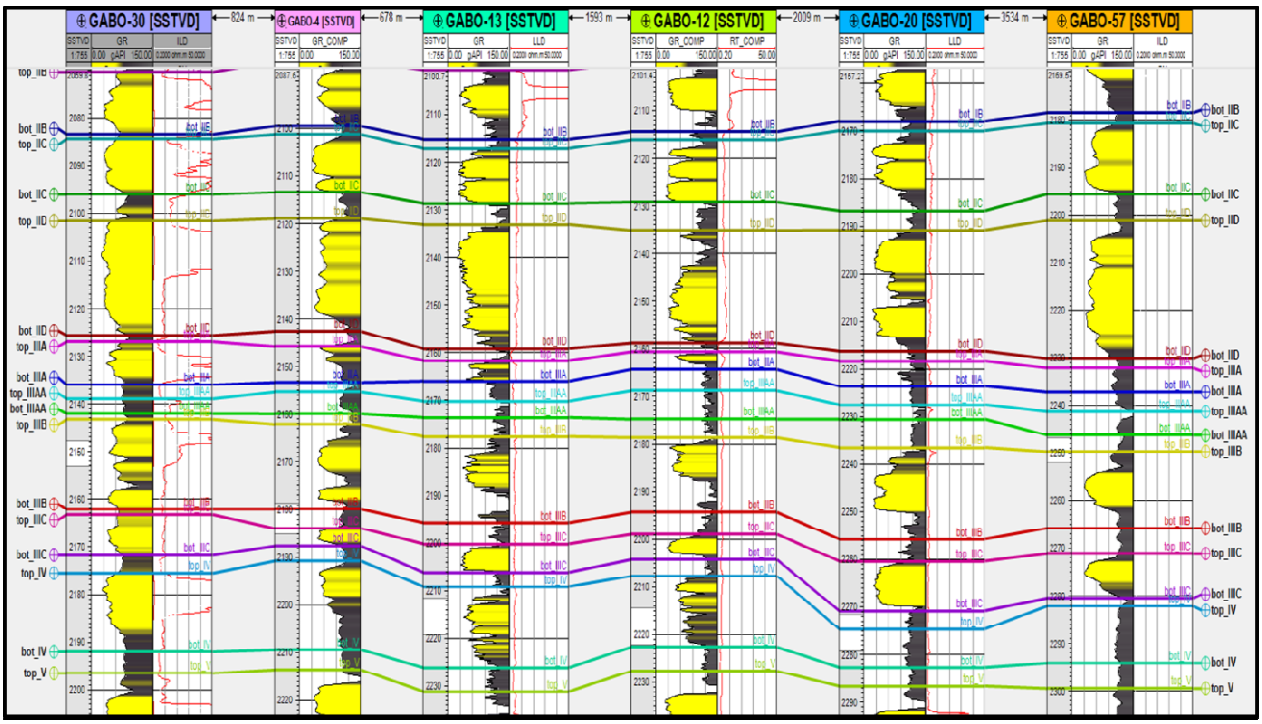

[illegible] Gabo well correlation along strike direction 3/5

NW **SE**

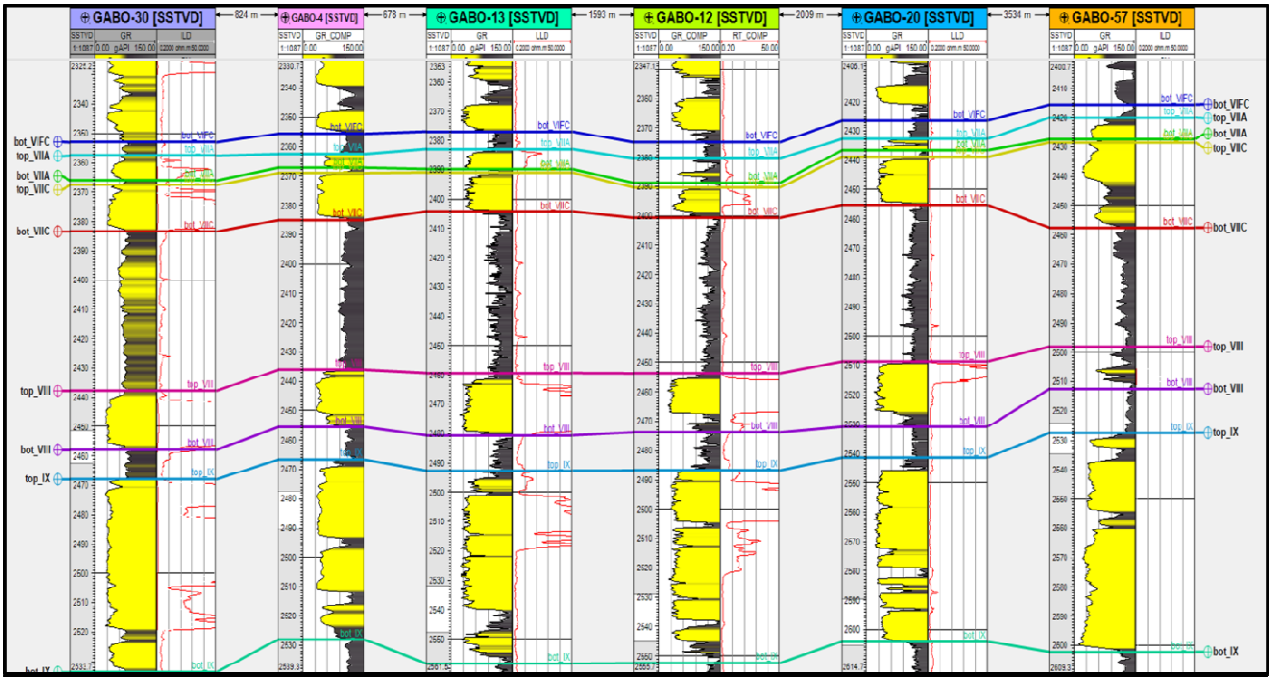

Fig 5d. Gabo well correlation along strike direction 4/5

NW **SE**

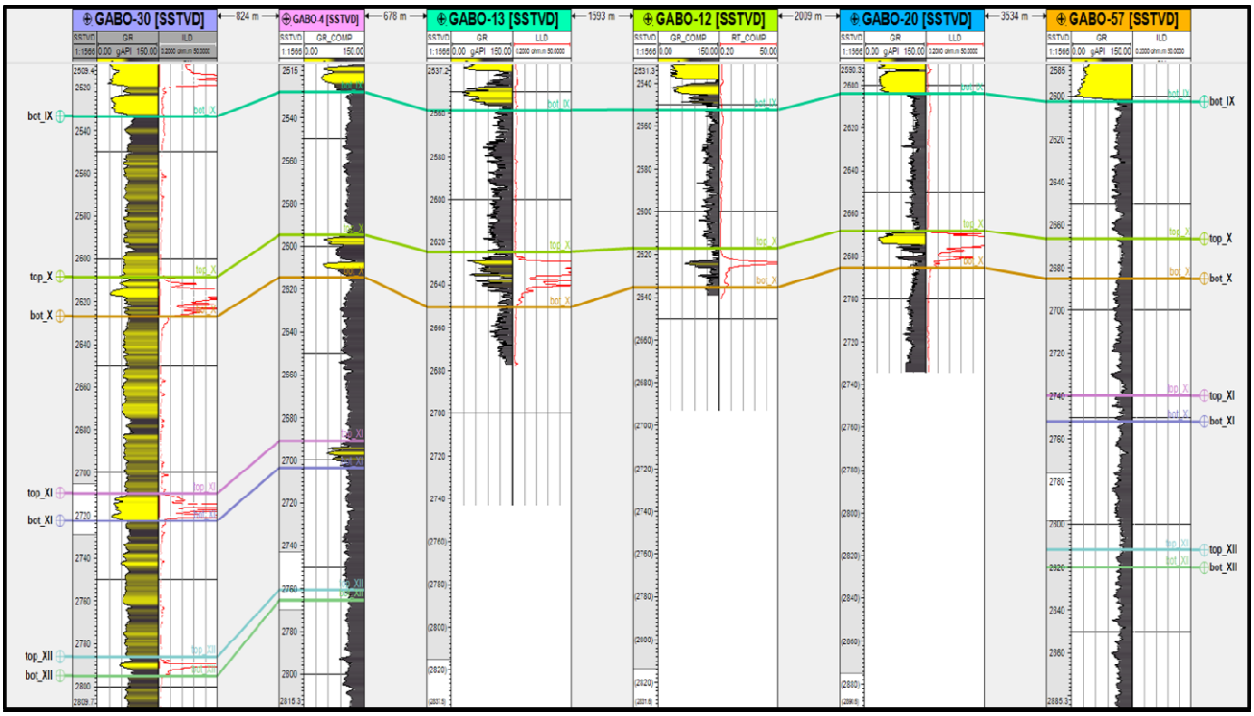

Figure 5e: Gabo well correlation along strike direction 5/5

B. Delineation of Reservoirs

Four (4) reservoirs A, B, C and D were delineated across the wells GABO 30, GABO 4, GABO 13, GABO 12, and GABO 20 respectively (Figures 6-9). This was achieved after analysis on motifs from gamma ray logs (GR) were used to delineate lithology and fluid characteristics were determined from the resistivity logs (R). As a result of this well log analysis, eight (8) horizons were picked which represents top and bottom of reservoirs A, B C and D across the wells in GABO field offshore Niger Delta (Fig 10).

NW **SE**

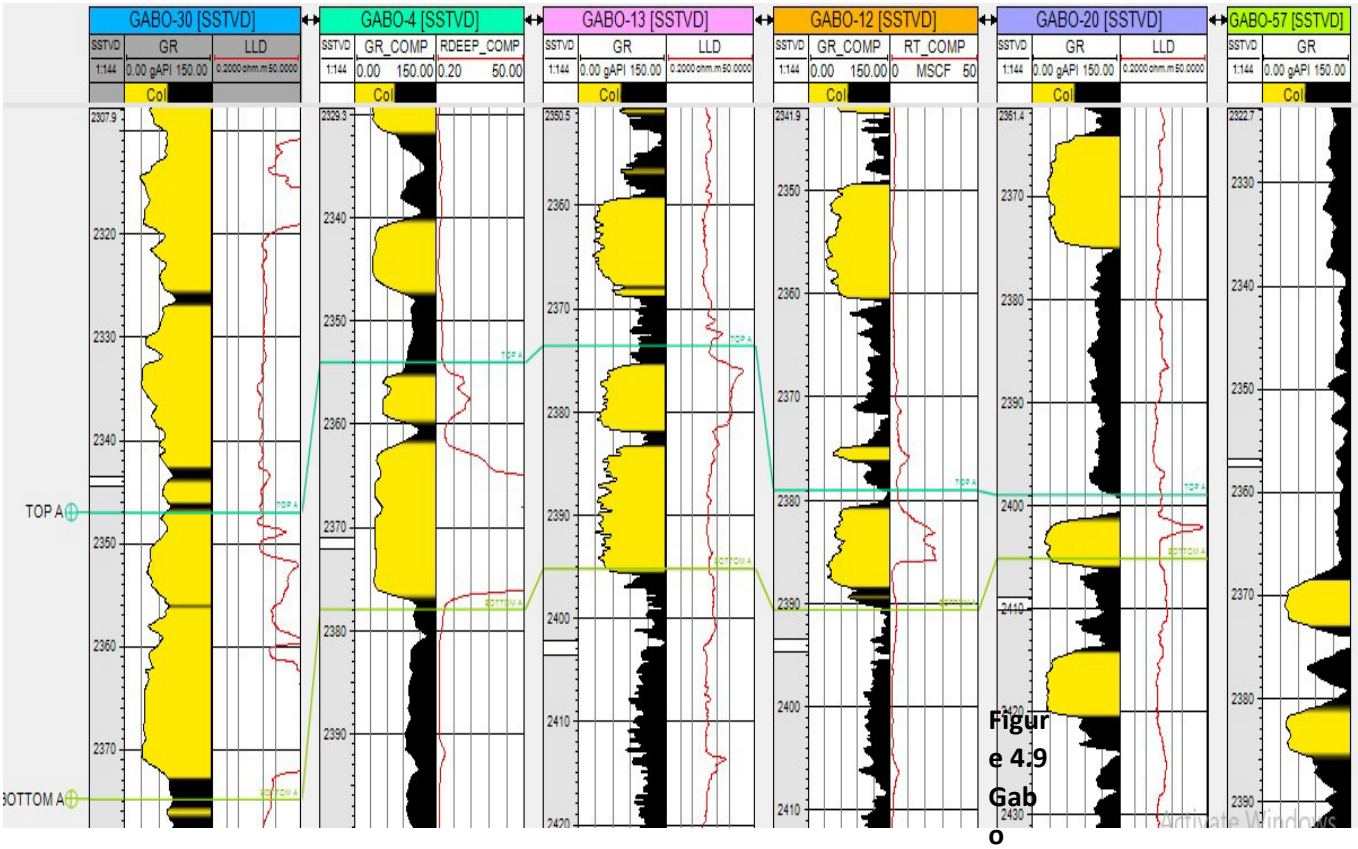

Fig 6: Gabo field reservoir A

Figure 4.9 Gabo field reservoir A

NW **SE**

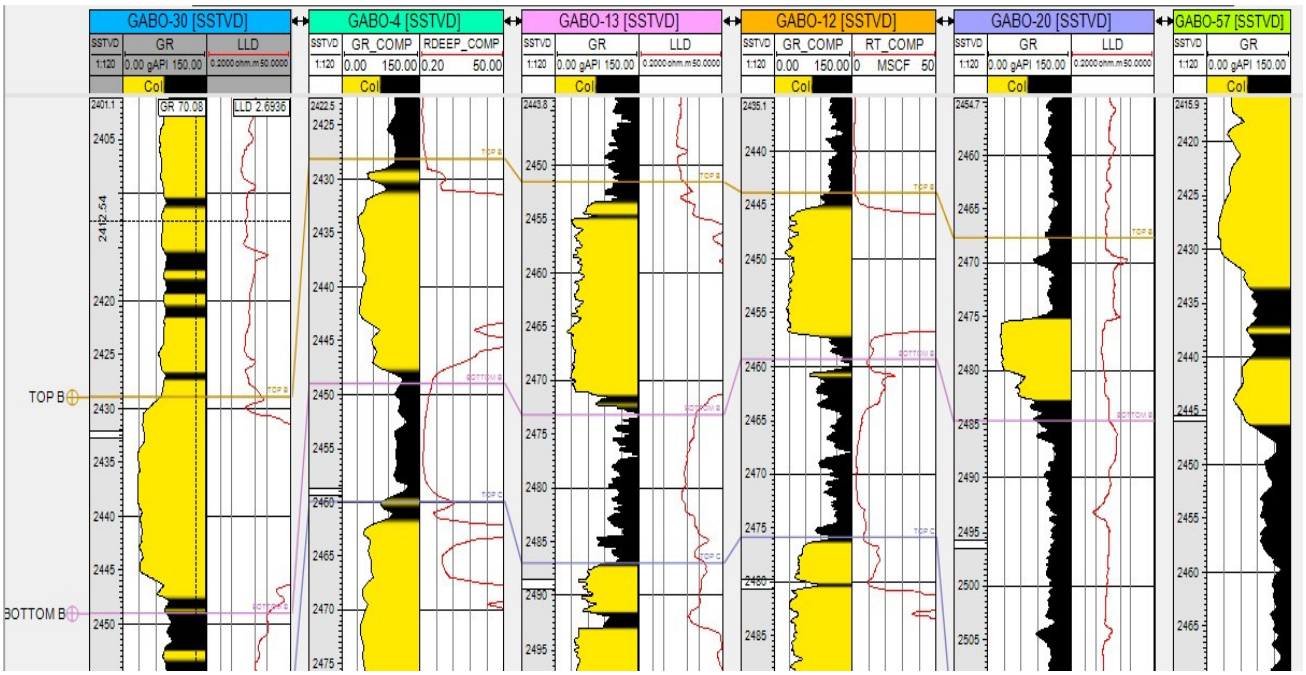

Fig 7. Gabo field reservoir B

NW **SE**

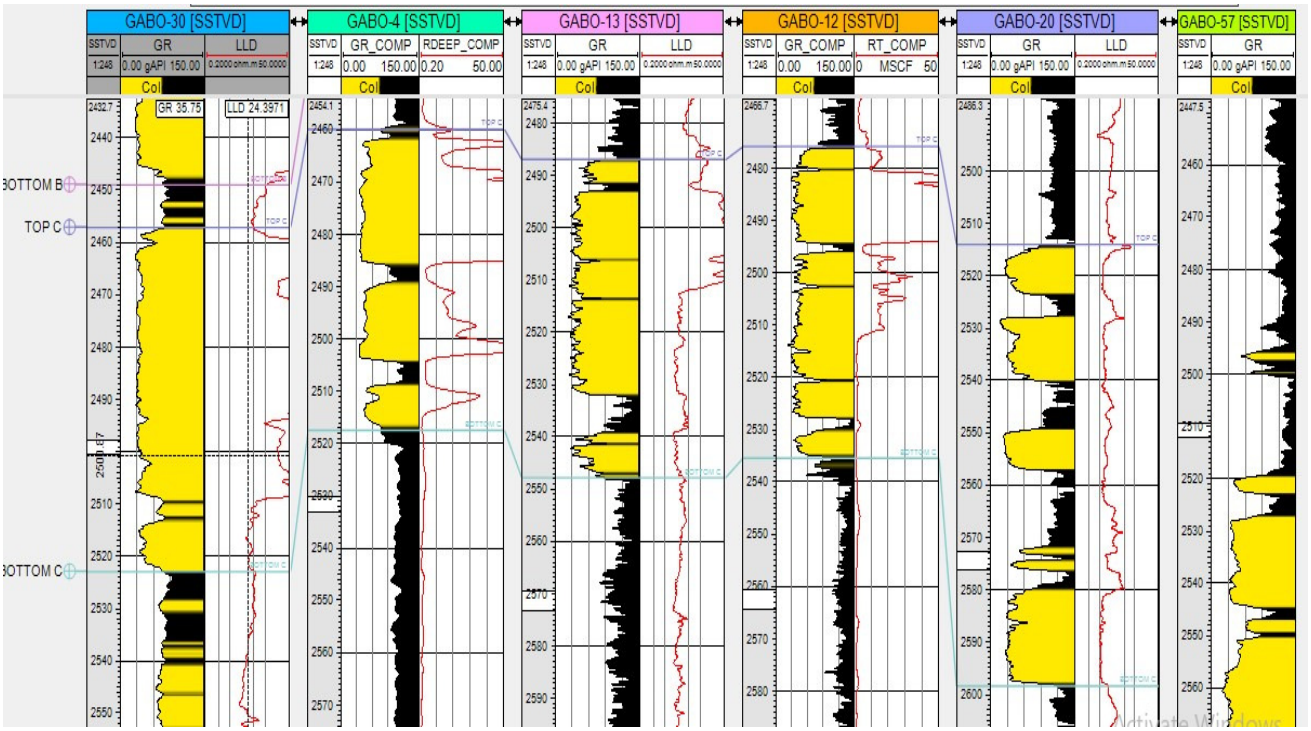

Fig 8: Gabo field reservoir C

SE

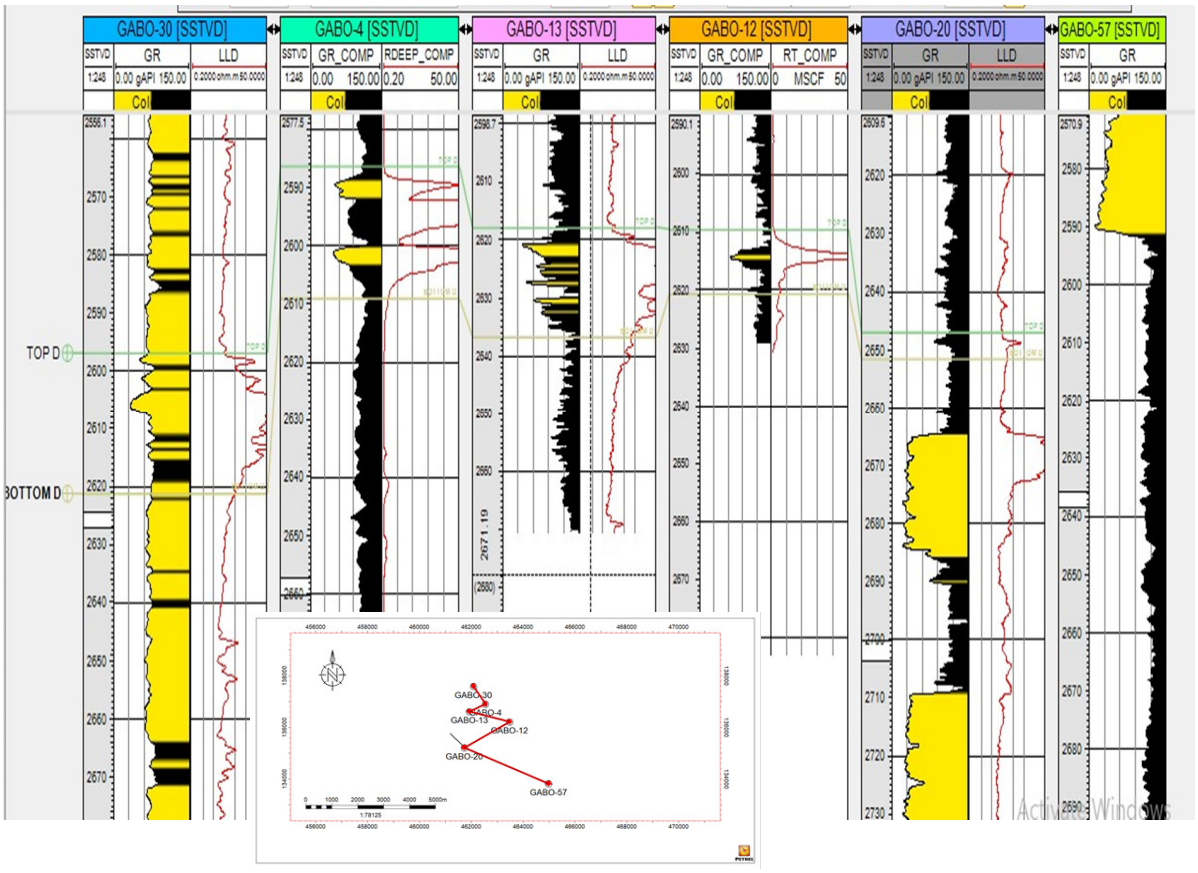

Fig 9: Gabo field reservoir D

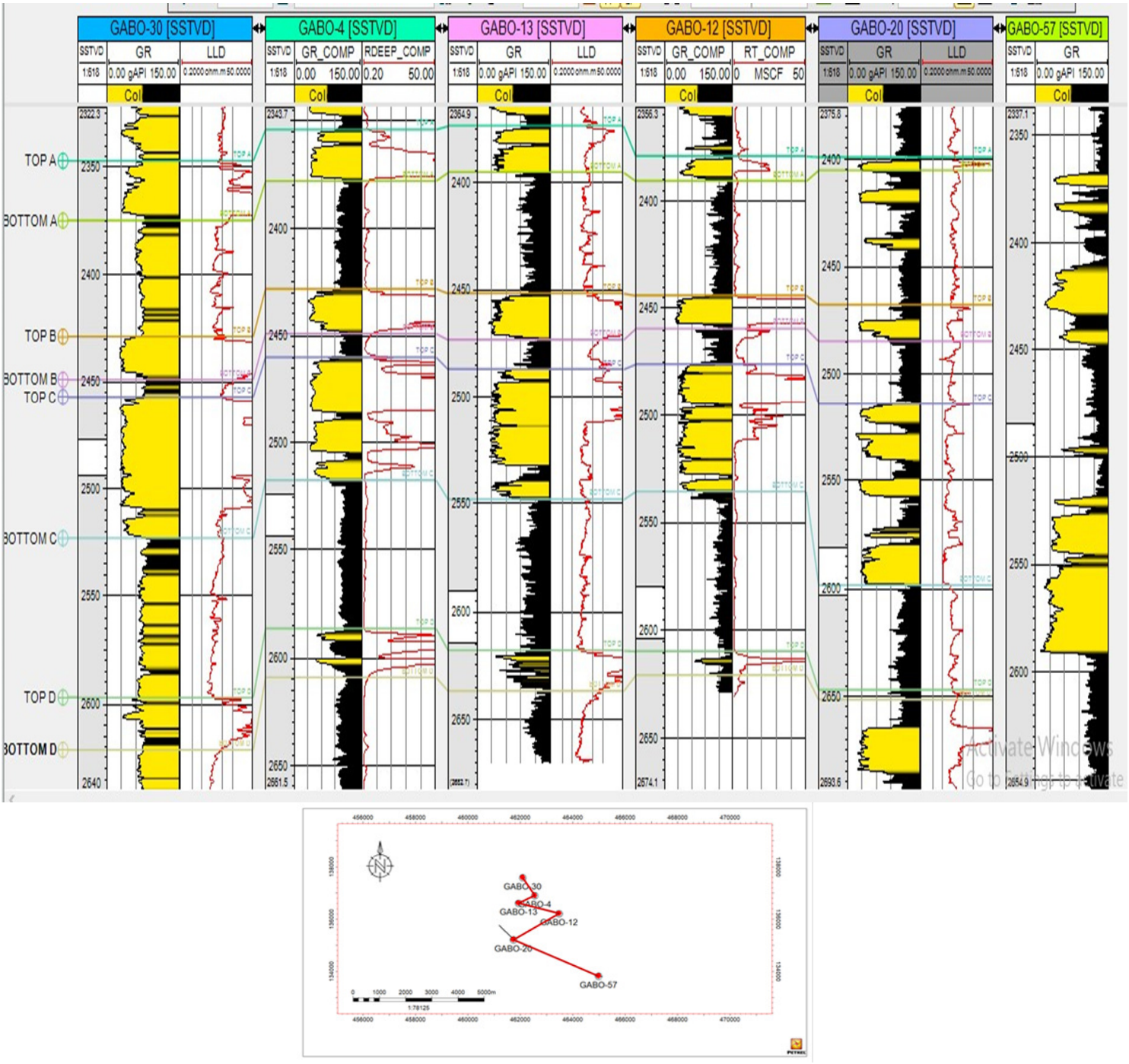

Figure 10: Correlation of Gabo well Reservoirs A, B, C and D

C.

Interpretation of Depositional Environments of identified Reservoirs from Gamma Ray Logs Motifs

The depositional environments of reservoir sands were interpreted from the analysis of shapes of gamma ray motifs. The inferred depositional environments of reservoir sands ranges from the fluvial channels, fluvial point bars, tidal point bar, deltaic distribution channels, delta fronts to upper shoreface depositional environments. Table 1 summarises the depositional environments of reservoirs inferred from gamma ray log motifs shapes.

Table 1: Depositional Environments of Reservoirs Inferred from Gamma Ray Log Motifs Shapes

S/N	Type of log motif shape	Reservoirs	Characteristics	Grain size	Inferred Depositional Environments
1	Cylindrical / Box Shape	Reservoir A-Part of well 13, part of well 4. Reservoir B-well 30, well 4, well 13 and well 12. Reservoir C-well 30, well 4, well 13 well 12, and parts of well 20	Sharp top and base with consistent trend	Relative consistent lithology	Fluvial channels, Tidal sands, Prograding delta distributaries.
2	Funnel Shape	Reservoir B-well 20. Reservoir D-well 4, well 13,	Abrupt top with coarsening	Grain size increases	Crevasse splay, River mouth bar, Delta front,

		and well 20	upward trend		Shoreface.
3	Bell Shape	Reservoir A-Part of well 30, and part of well 13	Abrupt base with finning upward trend	Grain size decreases	Fluvial point bar, Tidal point bar, Deltaic distributaries.
4	Symmetrical Shape / Bow Shape	Reservoir A-well 20 and, part of well 30. Reservoir B-well 30. Reservoir C-part of well 13, part of well 12 and part of well 20. Reservoir D-part of well 4, and part of well 12.	Ideally rounded base and top	Cleaning upward trend change into dirtying upward sequence from top	Transgressive shelf sands and mixed Tidal flat environment.

1. Cylindrical Shaped Gamma Ray Log Motifs

A number of eleven (11) beds across the reservoirs exhibited this gamma ray log characteristic, these are;

Reservoir A, part of well (Gabo)4

Reservoir A, Part of well (Gabo)13

Reservoir B, well (Gabo)30

Reservoir B, well (Gabo)4

Reservoir B, well (Gabo)13

Reservoir B, well (Gabo)12

Reservoir C, well (Gabo)30

Reservoir C, well (Gabo)4

Reservoir C, well (Gabo)13

Reservoir C, well (Gabo)12

Reservoir C, parts of well (Gabo)20

This motif is generally characterised by relatively constant values of gamma ray with sharp boundaries at the upper and lower limits which indicates a relatively uniform lithology, having an aggradation depositional pattern. This diagnostic motif is usually an indicative of fluvial channels, tidal sands, or deltaic distributaries channels depositional environments (Fig 11-13).

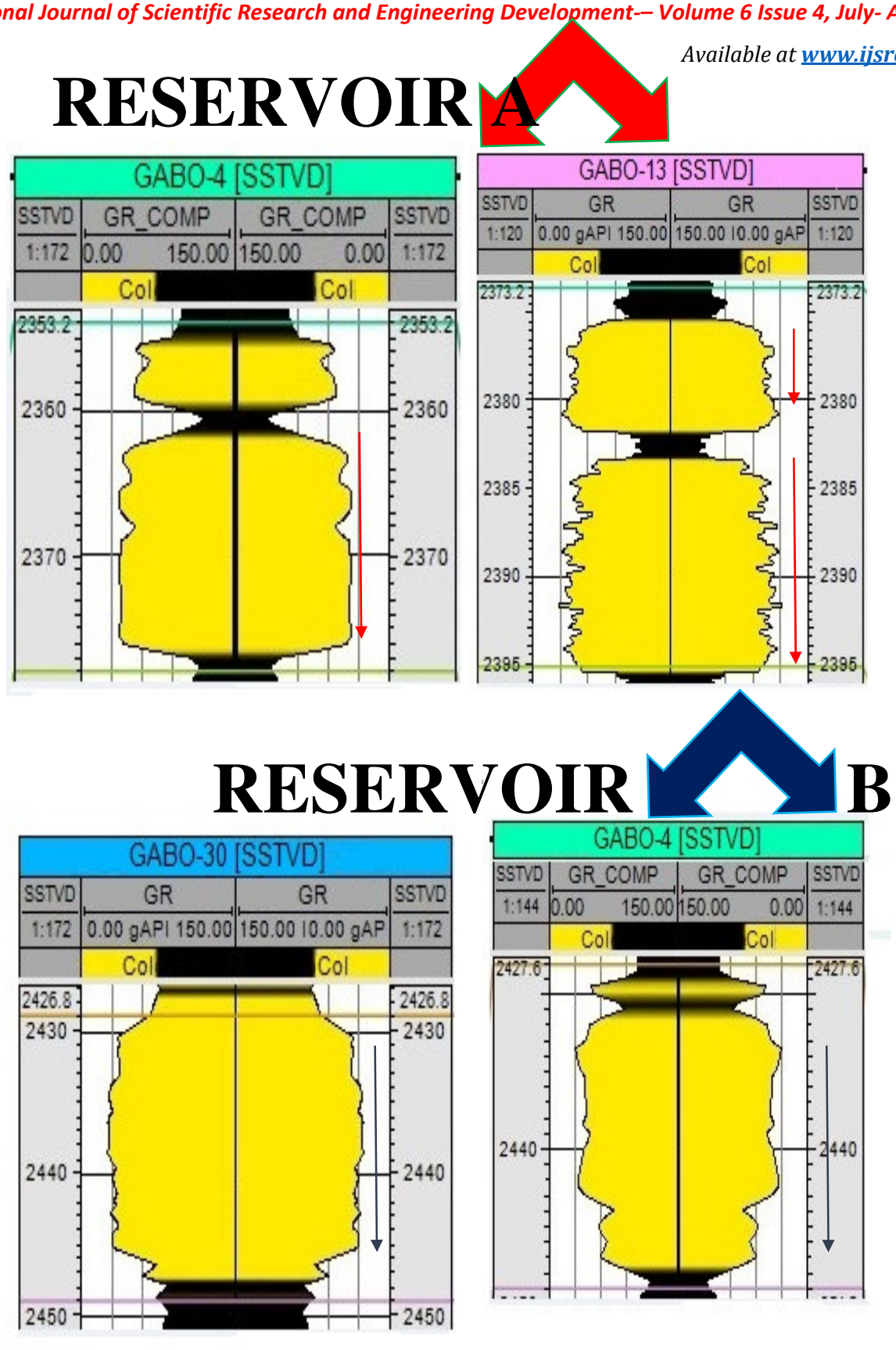

Fig 11: Cylindrical Shaped Gamma Ray Log Motifs across reservoirs A & B

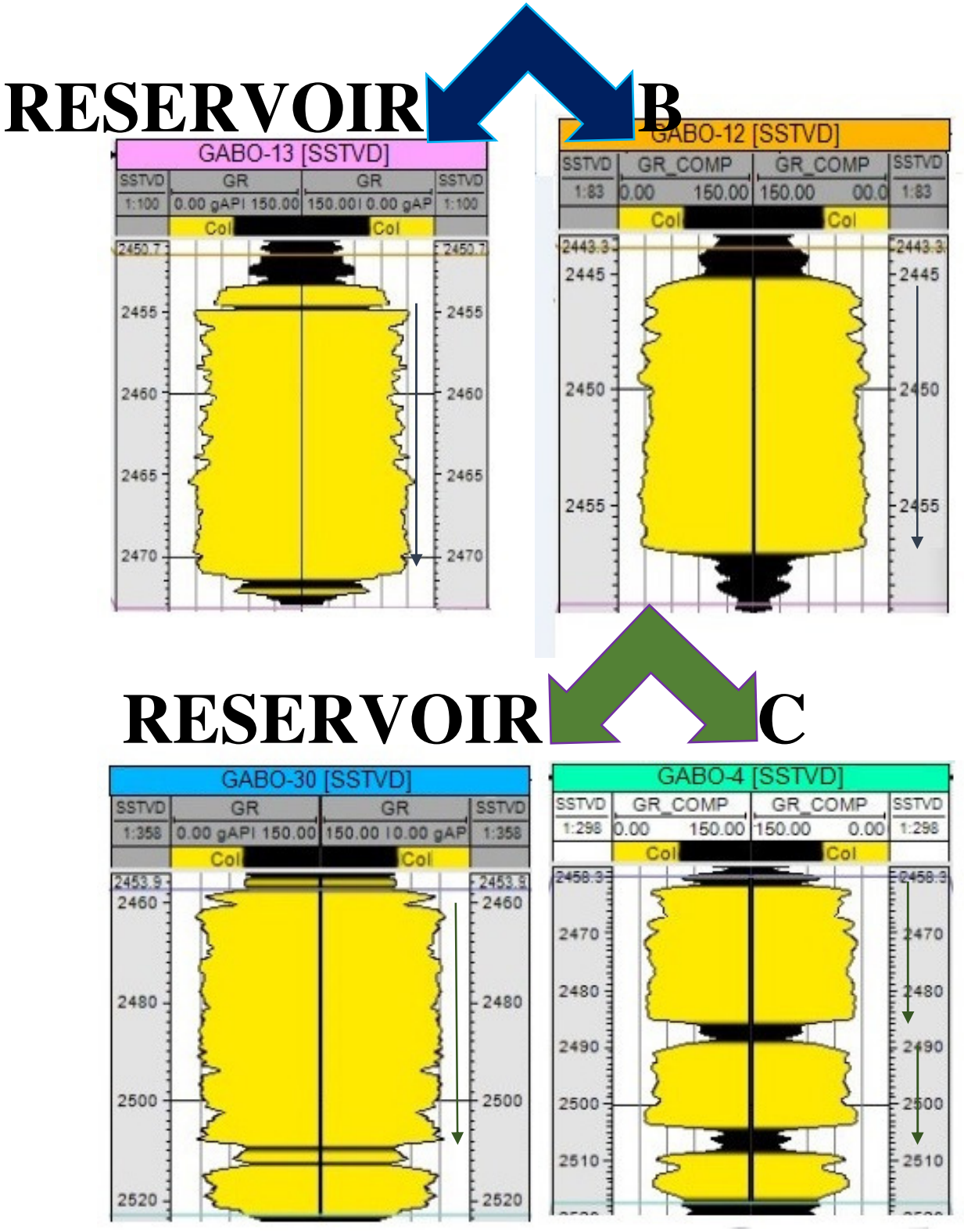

Fig 12: Cylindrical Shaped Gamma Ray Log Motifs across reservoirs B & C

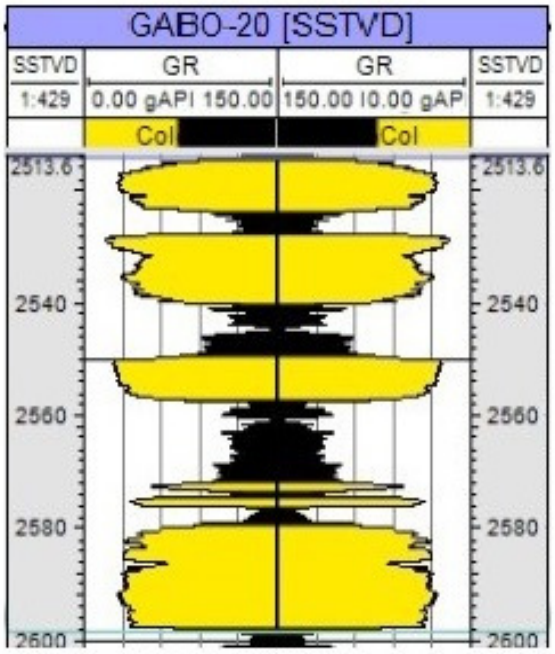

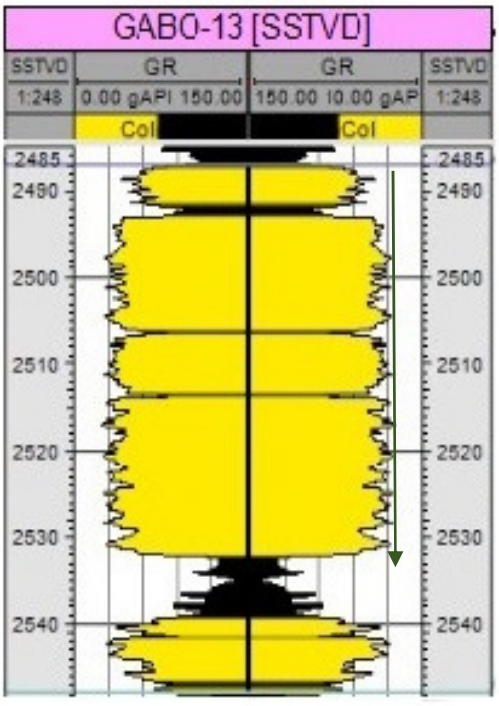

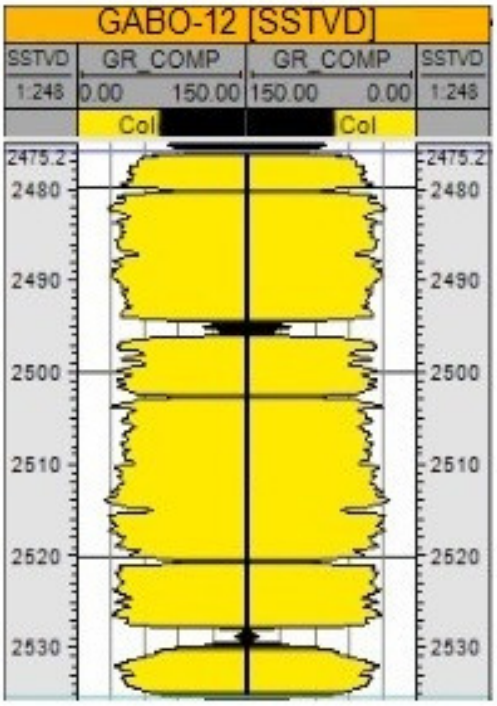

2. Funnel Shaped Gamma Ray Log Motifs

Four (4) beds in the delineated reservoirs exhibited this gamma ray log characteristic (figures 14 and 15), these are;

Reservoir B, well (Gabo) 20.

Reservoir D, well (Gabo) 4,

Reservoir D, well (Gabo) 13,

Reservoir D, well (Gabo) 20

This motif is generally characterised by a relatively decreasing values of gamma ray which indicates a decreasing shale content, increasing sands and also a coarsening upward (or cleaning upwards) depositional sequence. This diagnostic motif is usually an indicative of crevasse splay, river mouth bar, delta front or shoreface depositional environments.

RESERVOIR B

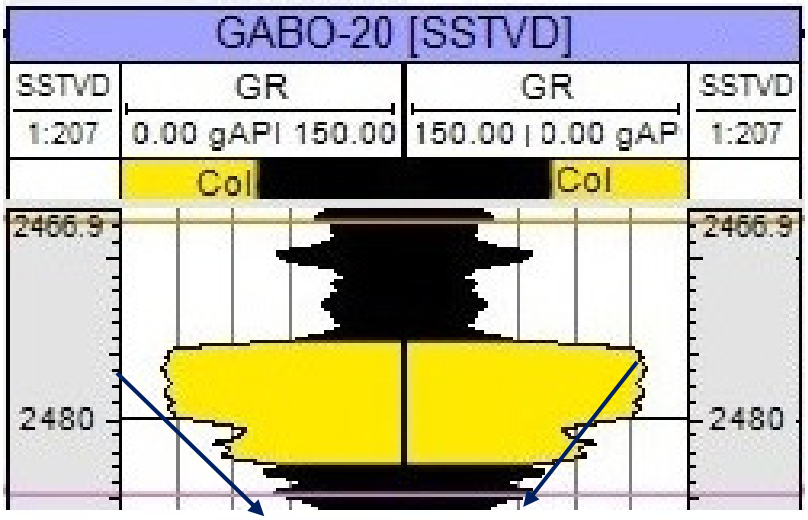

RESERVOIR D

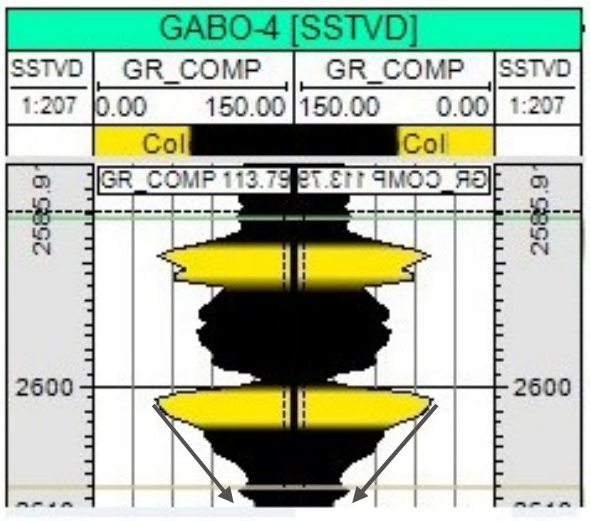

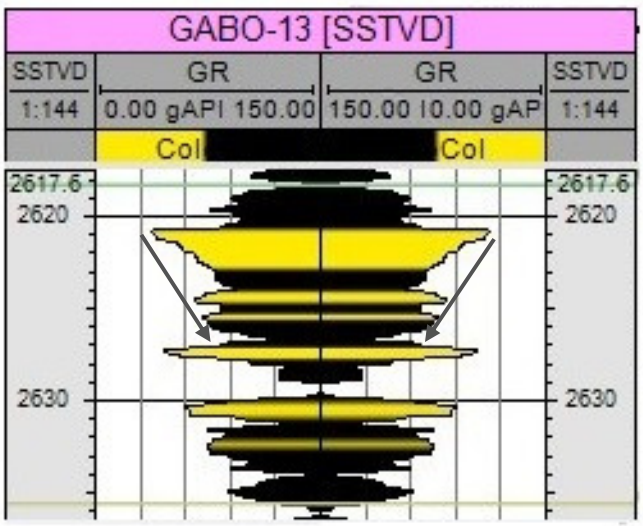

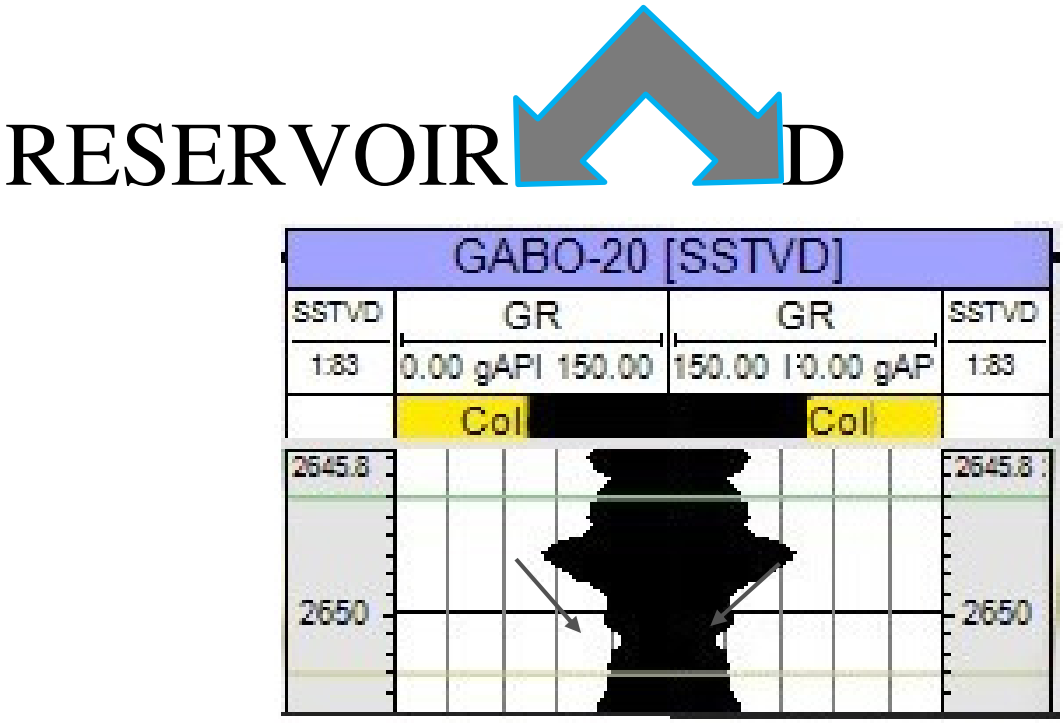

Fig 15: Funnel Shaped Gamma Ray Log Motifs across reservoir D

3. Bell Shaped Gamma Ray Log Motifs

Two (2) beds in the reservoirs exhibited this gamma ray log characteristic (fig 16). These are;

Reservoir A, Part of well (Gabo)30 and,

Reservoir A, Part of well (Gabo) 13

This motif generally shows an increasing upward values of gamma ray which indicates an increasing shale content and also a fining upward (or dirtying upwards) depositional sequence. This diagnostic motif is usually an indicative of fluvial channels, fluvial point bar, tidal channels, tidal point bar or deltaic distributaries channels depositional environments.

RESERVOIR A

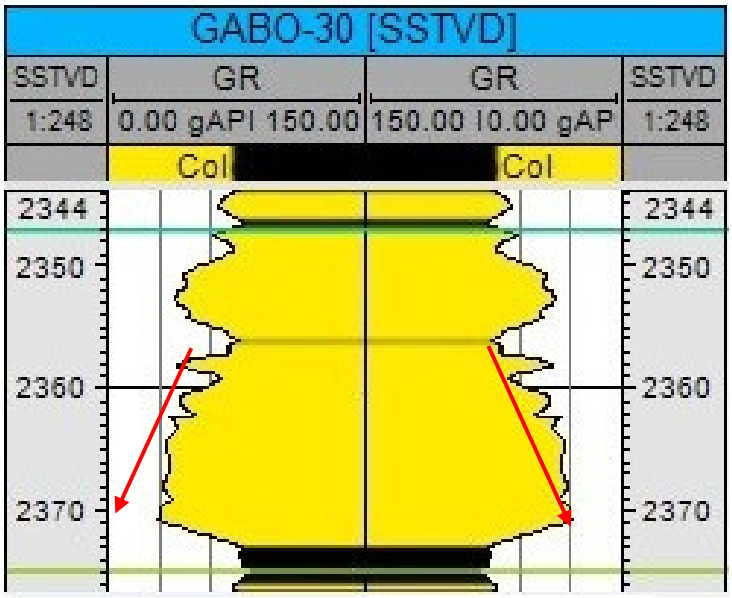

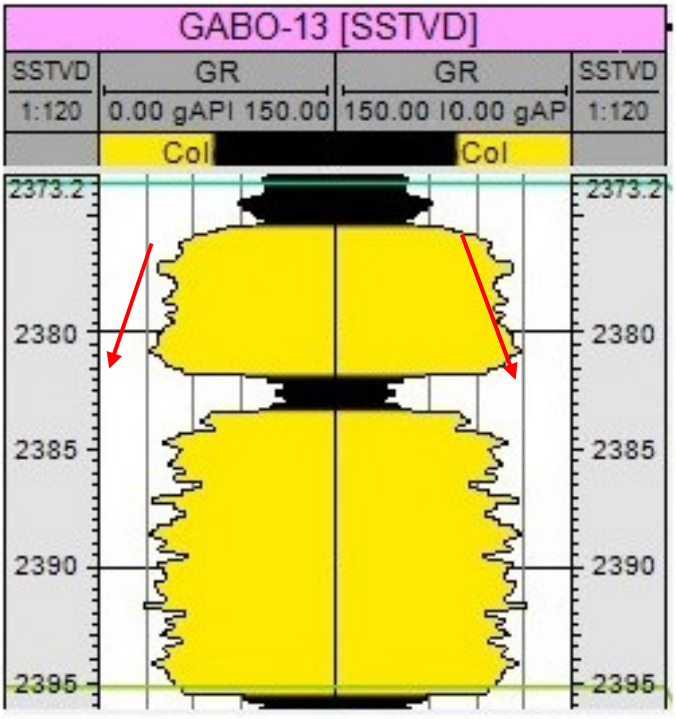

Fig 16: Bell Shaped Gamma Ray Log Motifs across reservoir D

4. Bow Shaped Gamma Ray Log Motifs

Seven (7) beds across the reservoirs exhibited this gamma ray log characteristic (fig 17 and 18), these are;

Reservoir A, well (Gabo) 20

Reservoir A, part of well (Gabo) 30

Reservoir C, part of well (Gabo) 13

Reservoir C, part of well (Gabo) 12

Reservoir C, part of well (Gabo) 20

Reservoir D, part of well (Gabo) 4

Reservoir D, part of well (Gabo) 12

This motif is generally characterised by a relatively increasing values of gamma ray followed by a relatively decreasing values of gamma ray which practically indicates a relatively increasing shale content (decreasing sands) followed by a relatively decreasing shale content (increasing sands) to form a bow shape depositional pattern. This diagnostic motif is usually an indicative of tidal channels sands or mixed tidal flats depositional environments.

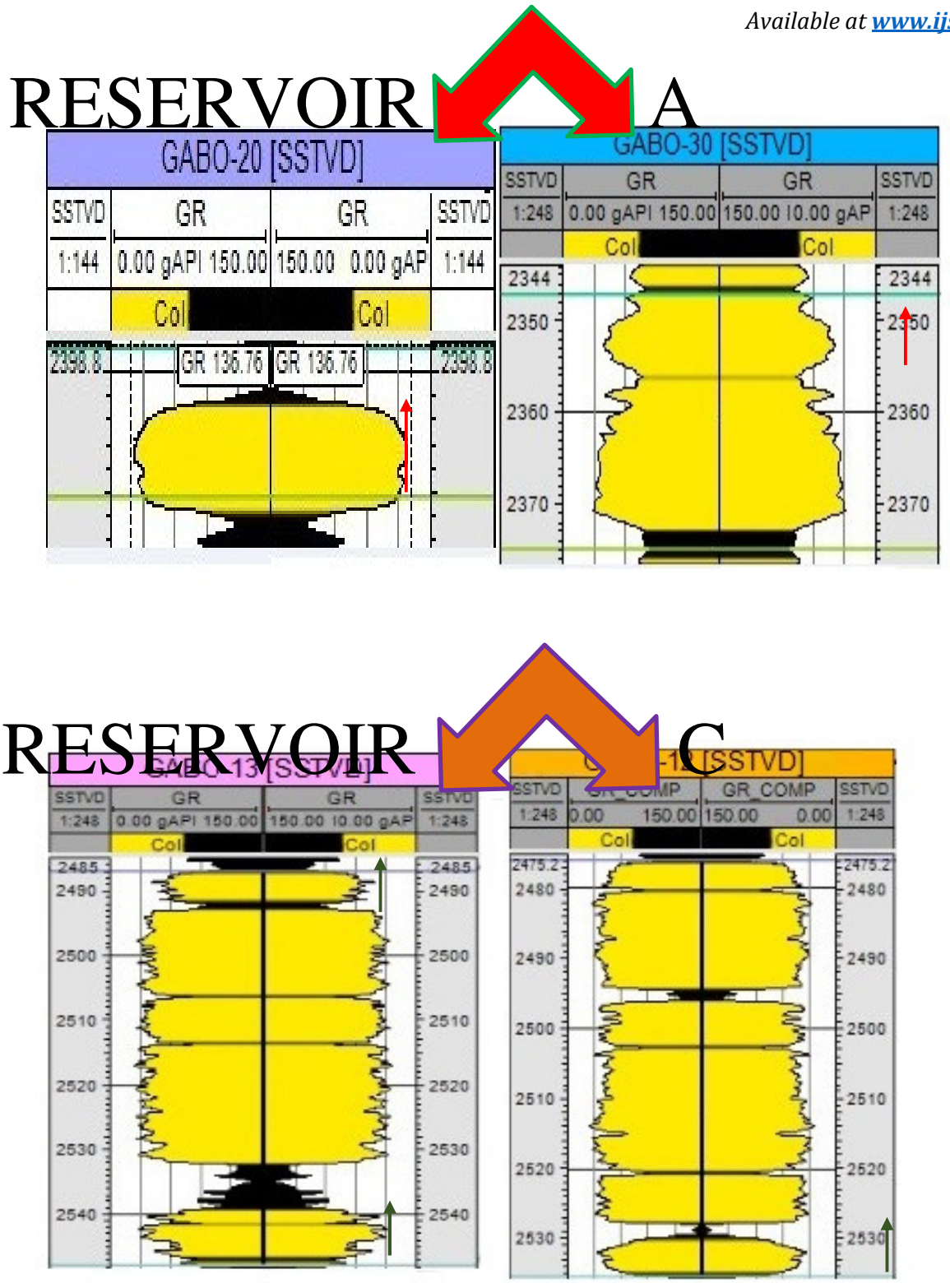

Fig 17: Bow Shaped Gamma Ray Log Motifs across reservoirs A and C

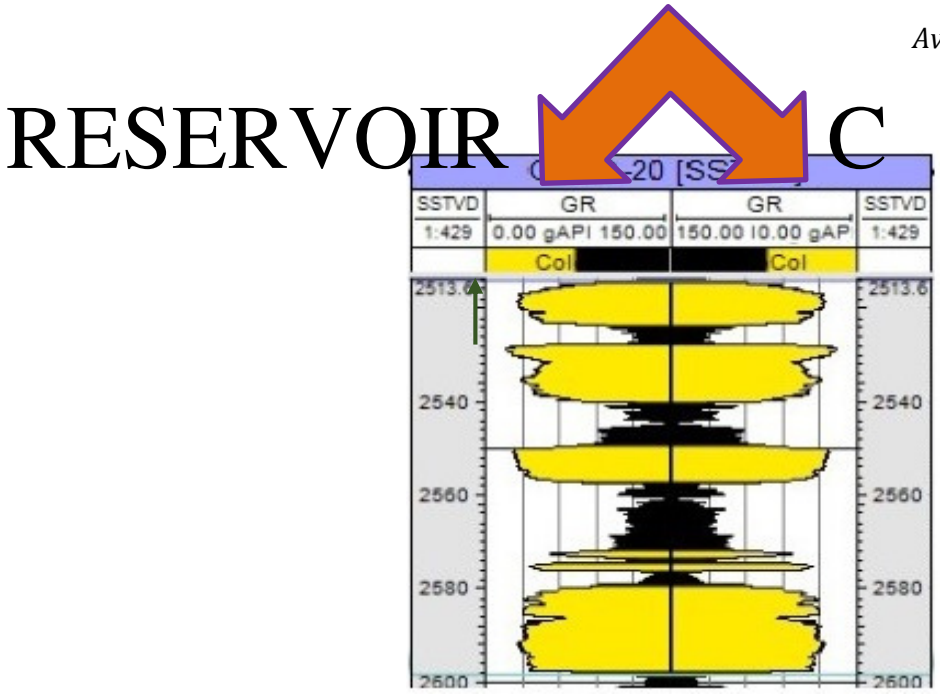

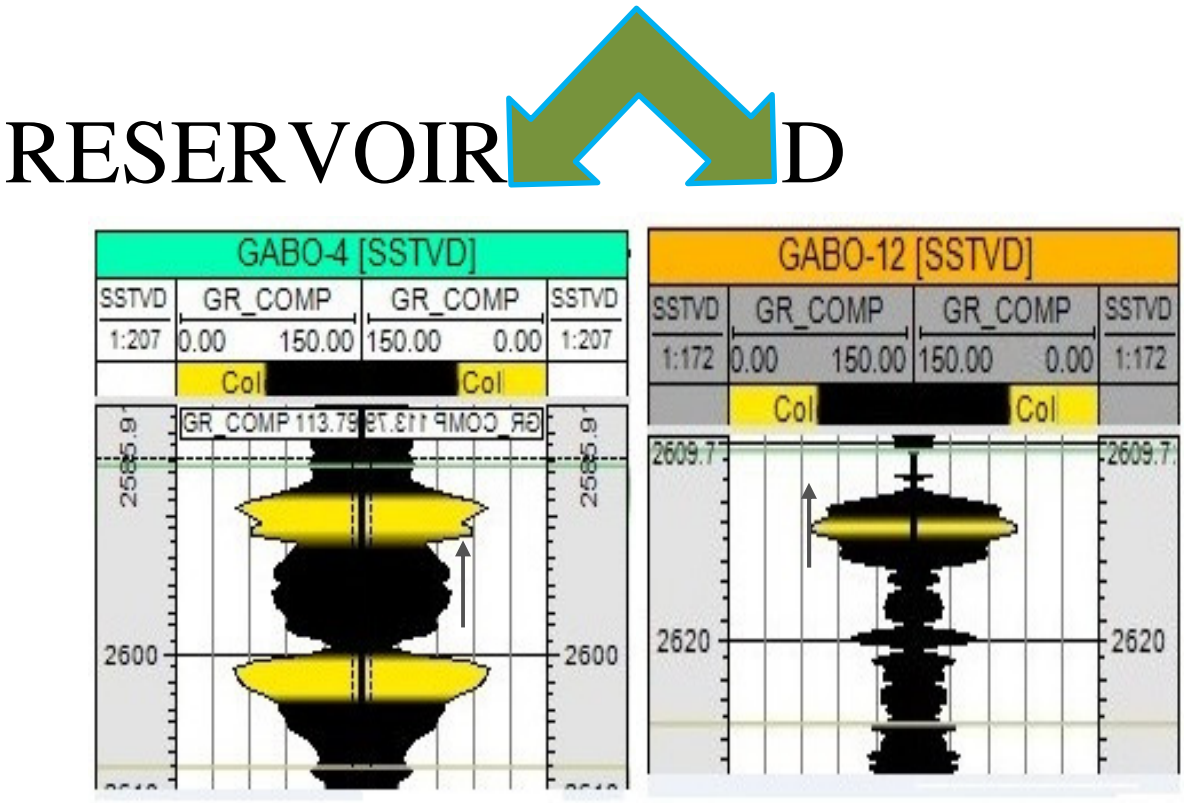

Fig 18: Bow Shaped Gamma Ray Log Motifs across reservoirs C and D

D. Generated Petrophysical Properties of Gabo field

Petrophysical analysis of Gabo field was carried out on all the wells except Gabo 57 because of its deficiency of Density (RHOB) and Resistivity logs respectively. Thus, Gabo 30, Gabo 4, Gabo 13, Gabo 12 and Gabo 20 has been analysed using density and resistivity logs to generate and delineate petrophysical properties across the wells. Petrophysical properties that were been generated include, volume of shale (vsh), total porosity (ϕt), effective porosity (ϕe), water saturation (Sw), hydrocarbon saturation (Sh) and permeability (mD).

The petrophysical properties that have been generated were limited to the reservoirs picked from the stratigraphic correlation of reservoir sand. In this research, four (4) reservoir have been picked which include Reservoir A, B, C, and D respectively, through which petrophysical analysis in this study has been carried out. The results of thepetrophysical analysis are presented in Tables 2 - 9.

Table 2. Top and Bottom depth intervals across the wells

WELL	Gabo 30	Gabo 4	Gabo 13	Gabo 12	Gabo 20
			DEPTH INTERVAL		
RESERVOIR A	2347.83	2354.78	2373	2375.34	2398.98
	2374.92	2377.57	2395.45	2390.85	2406.68
RESERVOIR B	2428.85	2427.85	2451.76	2443.81	2468.03
	2448.66	2448.63	2473.22	2457.9	2484.79
RESERVOIR C	2456.71	2459.36	2487.29	2475.99	2514.29
	2522.41	2517.07	2548.3	2566.66	2598.78
RESERVOIR D	2596.82	2586.07	2618.02	2610.07	2647.02
	2620.75	2586.07	2636.79	2620.8	2651.05

Table 3. Thickness of the reservoirs across the wells

WELL	Gabo 30	Gabo 4	Gabo 13	Gabo 12	Gabo 20
			THICKNESS		
RESERVOIR A	27.09	22.79	22.45	15.51	7.7
RESERVOIR B	19.81	20.78	21.46	14.09	16.76
RESERVOIR C	65.7	57.71	61.01	90.67	84.49
RESERVOIR D	23.93	0	18.77	10.73	4.03

Table 4. Average Shale volume (vsh) for each wells across the reservoir

WELL	Gabo 30	Gabo 4	Gabo 13	Gabo 12	Gabo 20
			AVG. SHALE VOLUME (%)		
RESERVOIR A	14.22	17.18	23.42	27.33	11.66
RESERVOIR B	9.97	12.87	14.53	21.34	40.42
RESERVOIR C	16.71	22.43	24.07	16.38	39.43
RESERVOIR D	24.6	50.4	47.93	75.33	93.68

Table 5. Average Total porosity (ϕt) for each well across the reservoir

WELL	Gabo 30	Gabo 4	Gabo 13	Gabo 12	Gabo 20
			AVG.TOTAL POROSITY (%)		
RESERVOIR A	38.71	21.89	23.37	18.52	17.32
RESERVOIR B	37.57	16.92	18.99	16.17	10.55
RESERVOIR C	35.72	28.06	23.3	24.84	20.81
RESERVOIR D	38.48	23.95	25.92	20.26	8.91

Table 6. Average Effective porosity (ϕe) for each well across the reservoir

WELL	Gabo 30	Gabo 4	Gabo 13	Gabo 12	Gabo 20
			AVG. EFFECTIVE POROSITY (%)		
RESERVOIR A	19.36	10.66	11.31	9.11	8.54
RESERVOIR B	18.79	8.3	9.27	7.9	5.2
RESERVOIR C	17.86	13.59	11.24	10.05	10.11
RESERVOIR D	19.24	11.73	12.74	10	4.4

Table 7. Average water saturation (Sw) for each well across the reservoir

WELL	Gabo 30	Gabo 4	Gabo 13	Gabo 12	Gabo 20

	AVG. WATER SATURATION (%)				
RESERVOIR A	48.81	64.11	62.95	70.99	77.6
RESERVOIR B	57.76	68.98	53.2	80.49	76.73
RESERVOIR C	19.98	30.92	48.88	54.47	90.82
RESERVOIR D	67.26	62.37	72.75	89.9	83.04

Table 8. Average hydrocarbon saturation (Sh) for each well across the reservoir

WELL	**Gabo 30**	**Gabo 4**	**Gabo 13**	**Gabo 12**	**Gabo 20**
	AVG. HYDROCARBON SATURATION (%)				
RESERVOIR A	51.13	35.89	37.06	44.11	22.4
RESERVOIR B	42.24	29.81	46.8	32.44	23.27
RESERVOIR C	80.02	69.08	51.27	16.81	9.18
RESERVOIR D	32.93	37.88	27.25	27.79	16.96

Table 9. Permeability (mD) attributes for each well across the reservoir

WELL	**Gabo 30**	**Gabo 4**	**Gabo 13**	**Gabo 12**	**Gabo 20**
	PERMEABILITY				
RESERVOIR A	1068.4	943.52	1000.7	798.4	746.8

RESERVOIR B	978.63	729.16	818.65	689.86	454.23
RESERVOIR C	966.35	1209.5	1004.2	1070.8	899.04
RESERVOIR D	1000.1	1028.9	1117.2	873.27	383.99

1. Petrophysical analysis for reservoir A

The depth range for the Tops of reservoir A has been picked from 2344.83ft – 2398.98ft across the wells, while the corresponding Bottom has been picked at 2374.92ft – 2406.68ft. All petrophysical attributes including, volume of shale (vsh), total porosity (ϕt), effective porosity (ϕe), water saturation (Sw), hydrocarbon saturation (Sh) and permeability(mD) have been generated and analysed in all the wells (Gabo30, Gabo 4, Gabo 13, Gabo 12, and Gabo 20) across the reservoir. The average thickness for reservoir A across the wells is 19.11ft.

A. Porosity Properties

Results from porosity crossplot (total porosity vs effective porosity) shows that the difference in porosity values across the wells is slightly negligible except for porosity results obtained in Gabo 30 (Figure 19). Although, crossplot of Gabo 30 can be traced through an imaginary linear line that connects all the wells in reservoir A, the large displacement between porosity crossplots of Gabo 30 and the rest wells signifies that Gabo 30 may have been drilled across a fault line or a fracture, or in addition, it could possibly mean that the density (RHOB) data obtained for well 30 was of suboptimal quality.

Porosity decreases with depth across the wells since crossplots for all the wells in reservoir A followed a linear scale. Furthermore, Gabo 12 has the least effective and total porosity values (although the margins are negligible) while Gabo 30 has the best porosity values across the wells in reservoir A, followed by Gabo 13 and Gabo 4. The estimated average effective porosity of reservoir A across the wells is 11.80% while the average total porosity of reservoir A is approximately 23.96%

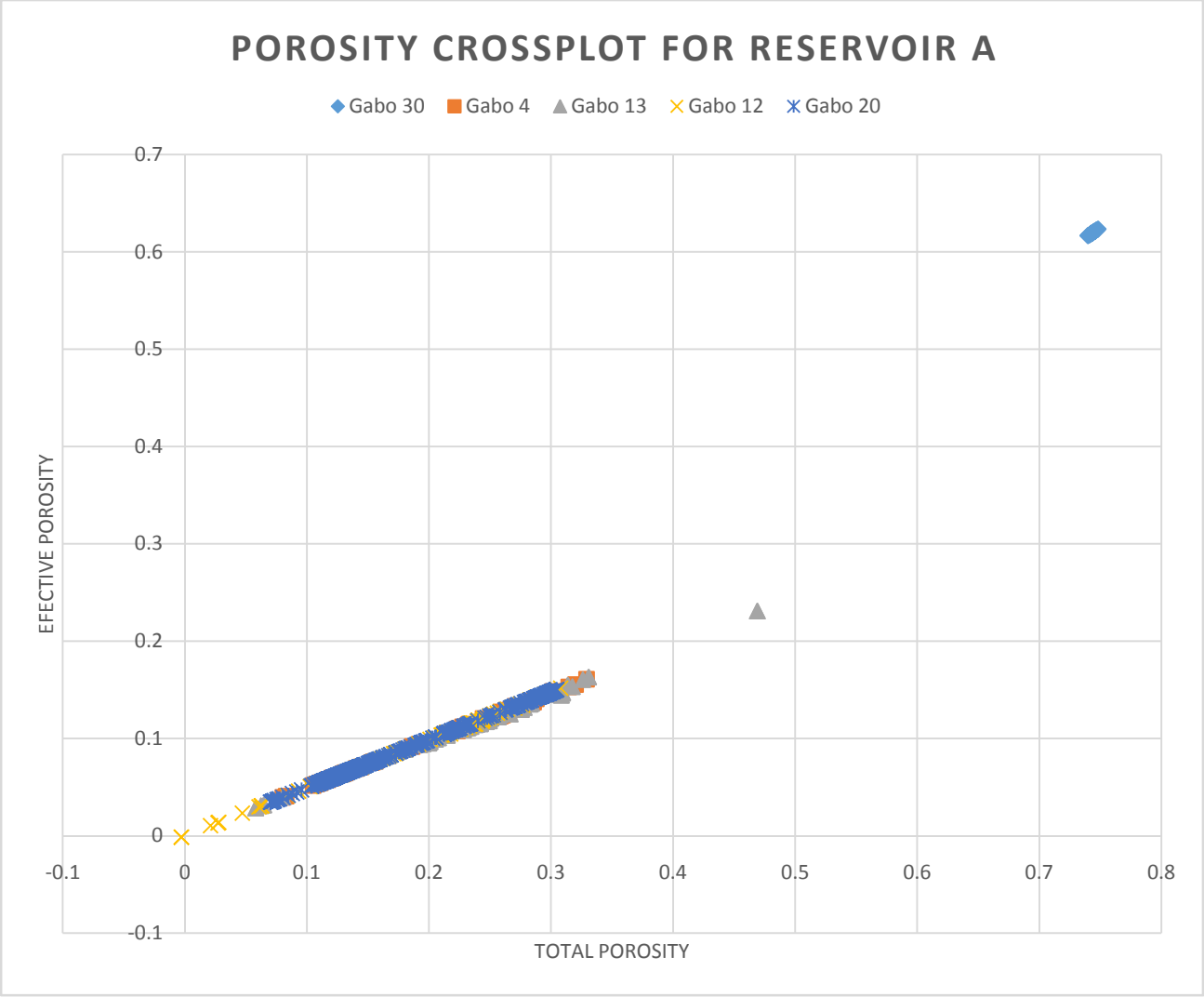

Fig 19. Porosity crossplot for reservoir A

B. Plot of Depth against Permeability for Reservoir A

Permeability of reservoir A across the wells shows a heterogeneous trend for all

the wells unlike what was delineated in the porosity crossplot across the wells. For Gabo 30, permeability maintained a steady value as depth increases. This could be indicative of a fracture, a joint or a bad geophysical density (RHOB) data. While permeability increases with depth in Gabo 4, Gabo 13 and Gabo 20, it showed a decreasing trend with depth in Gabo 12 (Figure 20). The average permeability reading across reservoir A is 911.56mD. From reference [8] porosity and permeability classification, the qualitative description of reservoir A's porosity is 'good', as well as having a 'very good' permeability property or value.

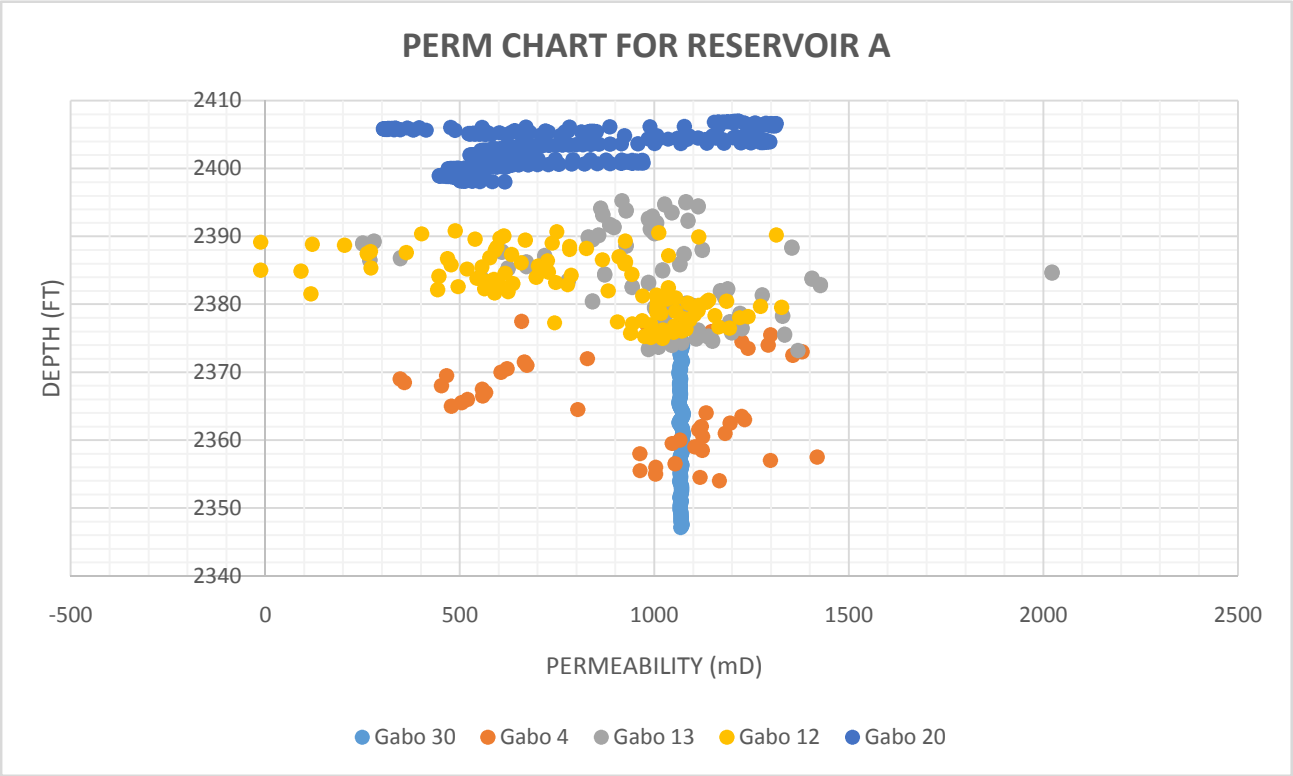

Fig 20. Permeability chart for reservoir A

C. Fluid saturation attributes

Water saturation (Sw) and hydrocarbonsaturation (Sh) crossplots shows a fairly homogeneous linear aggregate of values in Gabo 4, Gabo 13 and Gabo 20 (Figure 21). The aforementioned attribute is indicative of a linear reduction of fluid saturation with depth in reservoir A across the wells of interest. For well 12, water saturation (Sw) and hydrocarbon saturation (Sh) crossplot attributes forms a semi concave curve above the best fit exponential line as it deviates significantly from the latter. This is indicative of a fairly high fluid saturation that has more water fractions than hydrocarbon content. Although Gabo 30 appeared chaotic, it fairly followed the best fit exponential trend.

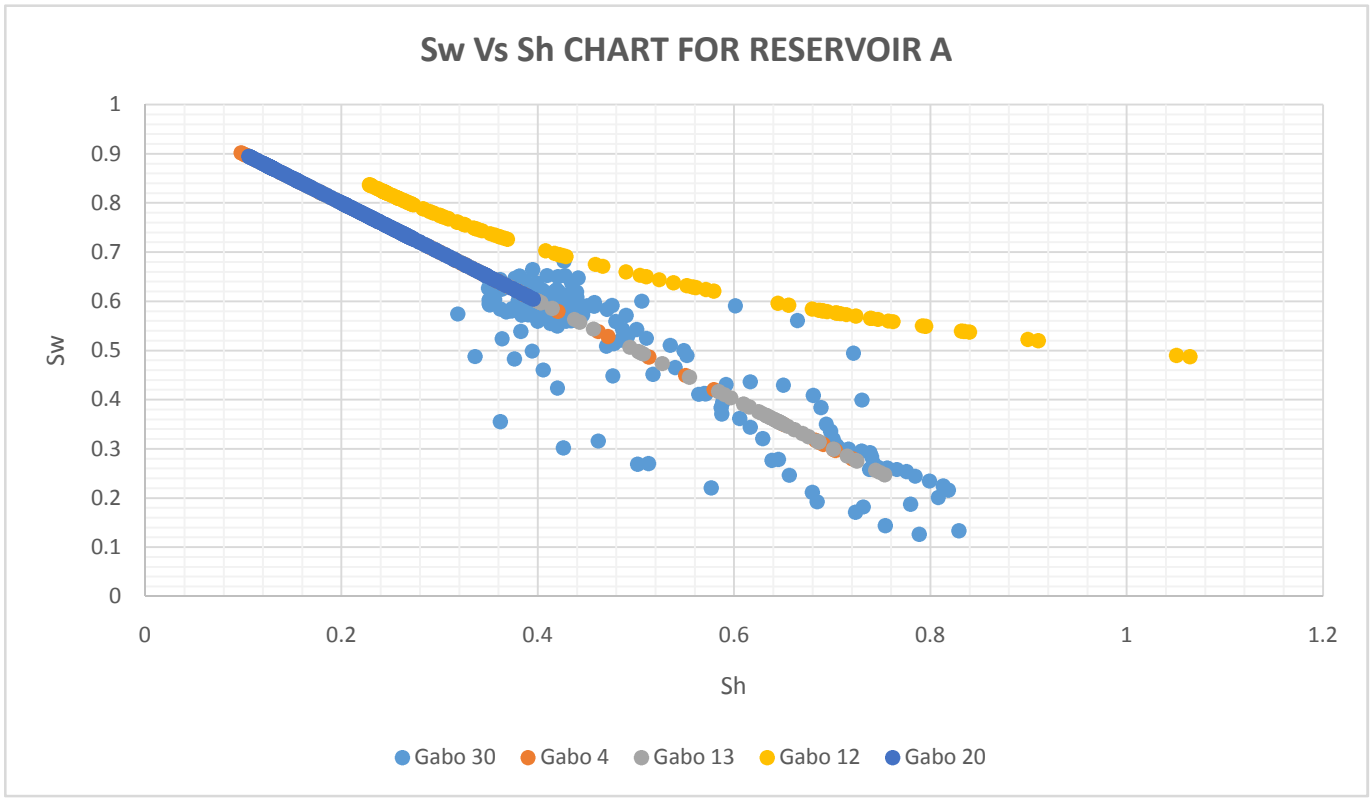

Fig 21. Crossplot of water saturation (Sw) vs hydrocarbon Saturation (Sh) chart for reservoir A

2. Petrophysical analysis for reservoir B

The average thickness for Reservoir B across the wells is 18. 58ft. Reservoir B has stratigraphic Top values (in depth) ranging from 2427.85ft – 2468.03ft across the wells while its stratigraphic Bottom values ranges from 2448.63ft – 2484.79.

A. Porosity attributes

Result of total porosity vs effective porosity crossplots (Figure 22) shows that porosity followed a linear regression line which signifies that porosity values decreases with depth across the wells in reservoir B. Similarly, there is huge graphical semblance of porosity crossplots of reservoir A and reservoir B in which the displacement of porosity magnitudes between the wells has been negligible except for crossplot values of Gabo 30, which has significant high total and effective porosity values. Also apart from Gabo 30, Gabo 13 has been identified as having the highest porosity value thus, this signifies that the latter is more porous than the others. Gabo 4 and Gabo 12 have significant high porosity properties next to Gabo 13. Gabo 20 has been identified as having the least porosity values in reservoir B. Average total porosity of reservoir B has is of 20.04% while that of effective porosity is 9.89%. Following reference [8] porosity calculation, reservoir B has been classified to having good to very Good porosity attributes

.

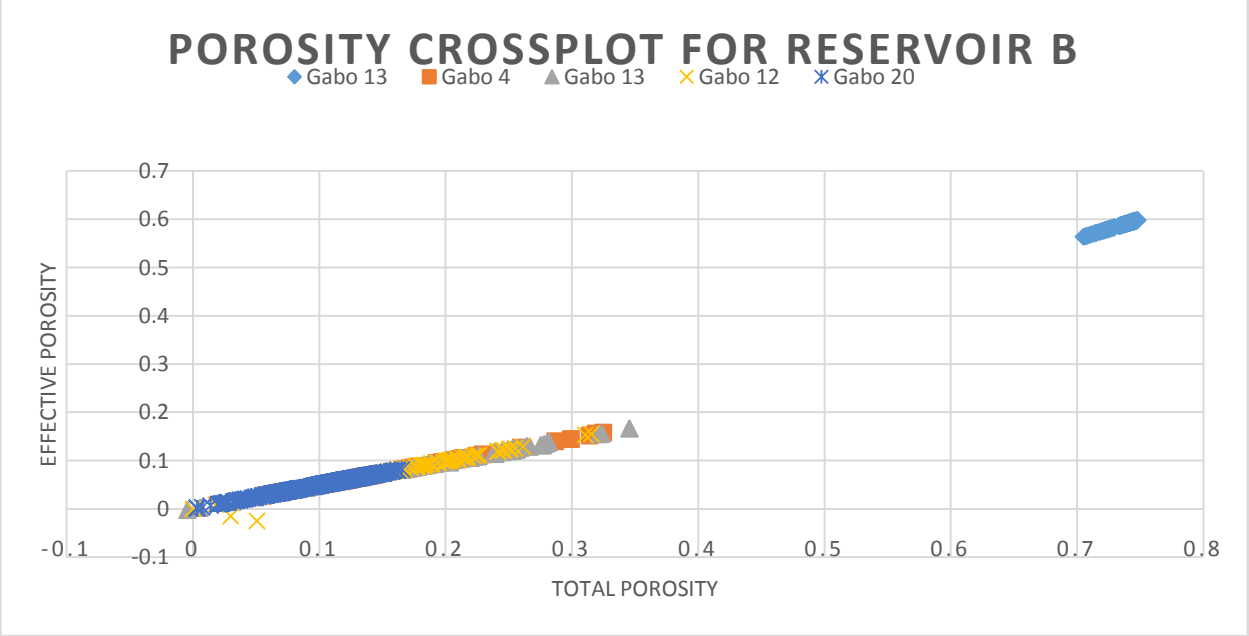

Fig 22. Porosity crossplot for reservoir B

B. Permeability attributes

Unlike reservoir A, permeability chart tends to follow a more a more visible homogeneous trend, except permeability values of Gabo 30. Almost all the permeability values across the wells increases with depth except for Gabo 30 which appeared to have maintained a steady permeability value as depth increases. This visibly delineated as a vertical line on the permeability chart in Figure 23. In comparison, permeability results obtained in reservoir B showed that reservoir A has suboptimal transmissivity properties compared to reservoir B. Although the magnitude of permeability between wells in reservoir B looks fairly negligible except for those of Gabo 30. Gabo 20 appears to have the highest values of permeability. The estimated average permeability across wells in reservoir B is 734.11mD which signify a 'very good' rating according to reference [8] permeability classification.

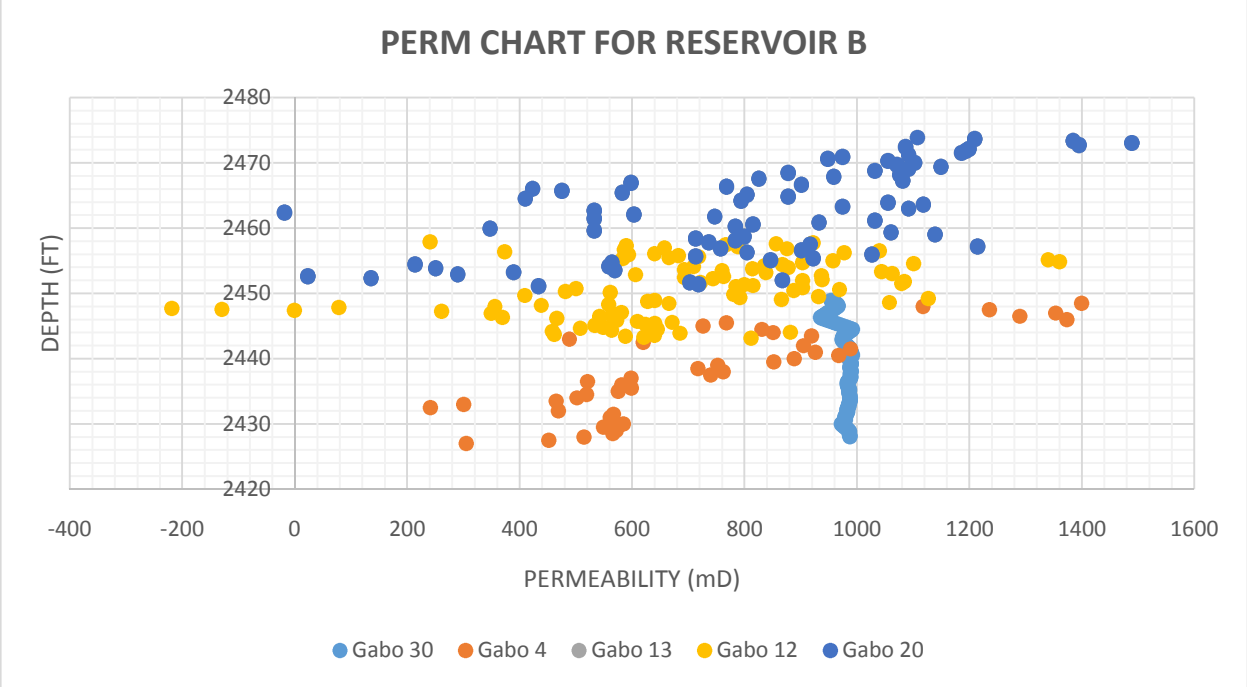

Figure 23. Permeability chart for reservoir B

C. Fluid saturation attributes

Water saturation (Sw) and hydrocarbon saturation (Sh) crossplot (Figure 24) shows a well-defined graphical attribute of fluid saturation of reservoir B. While all the values of water and hydrocarbon saturation formed a diagonal linear line (which often deputizes as the exponential best fit line) and depicts reduction in fluid saturation with depth for the wells associated, those associated with Gabo 12 follows a similar concave curve just above the exponential best fit line for Sw and Shcrossplot.

The graphical representation of Gabo 12 in substantiates that it possesses more fluid saturation and contains more water than hydrocarbon. While Gabo 30 and Gabo 12 has been attributed to containing high hydrocarbon saturation to water saturation, the rest wells exhibit fairly the opposite.

Fig 24. Crossplot of water saturation (Sw) vs hydrocarbon Saturation (Sh) chart for reservoir

3. Petrophysical analysis for reservoir C

Reservoir C has been picked from Top to Bottom across the wells having a corresponding depth range of 2456.71ft – 2514.29ft for Tops as well as 2517.07ft – 2598.78 for reservoir Bottoms. The average thickness of this reservoir is 71.92ft, making it the largest hydrocarbon reservoir in the field. Just like reservoirs A and B, all petrophysical attributes including volume of shale (vsh), total porosity (ϕt), effective porosity (ϕe), water saturation (Sw), hydrocarbon saturation (Sh) and permeability(mD) has all been analysed across the wells (Gabo30, Gabo 4, Gabo 13, Gabo 12, and Gabo 20) in the reservoir.

A. Porosity attributes

Results from total porosity and effective porosity crossplot in reservoir C (Fig 25) has been propagated along a straight linear regression line that depicts decreasing porosity with depth. Gabo 30 has the highest magnitude of porosity values across the wells while Gabo 20 appears to have larger lateral extent of porosity with depth. Lastly, the displacement of porosity values across Gabo 4, Gabo 12 and Gabo 13 has been fairly negligible. Average total porosity of reservoir C stands at 26.54%, while that of effective porosity is 12.57%, thus signifying that reservoir C has good to very good porosity attributes[8].

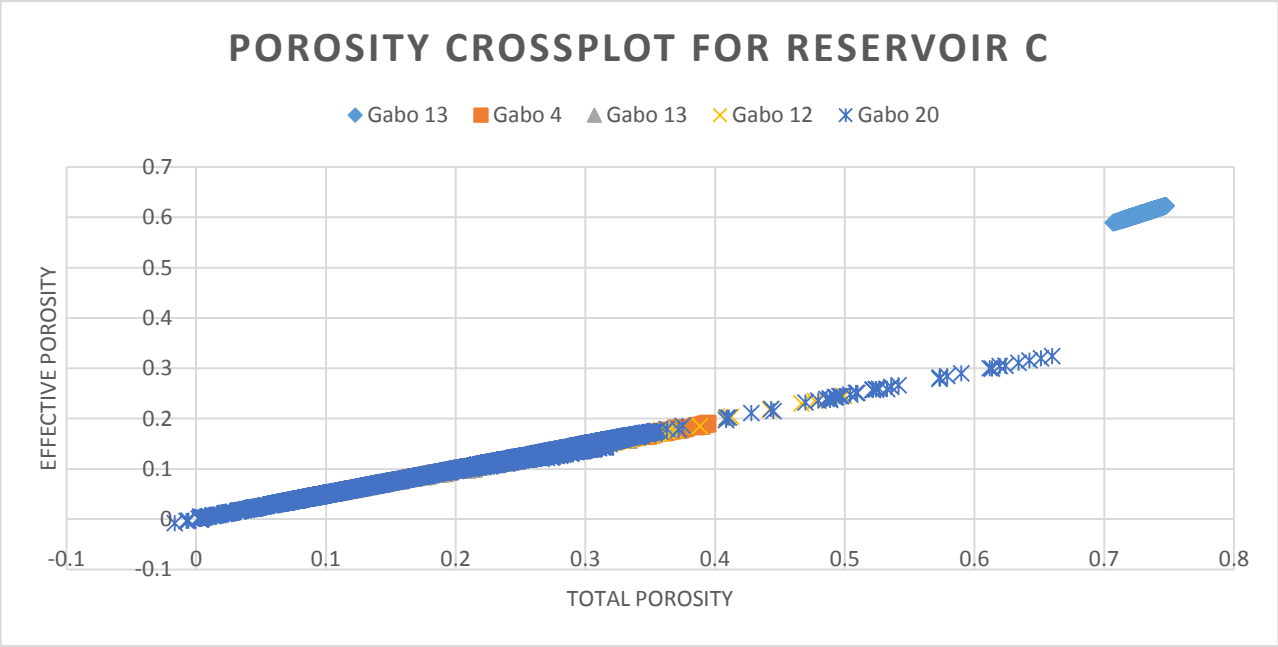

Fig 25. Porosity crossplot for reservoir C

B. Permeability attribute

The Result, figure 26 shows that permeability values maintained a static or slightly increasing trend with depth across the wells. Gabo 4, Gabo 12 and Gabo 20 has been substantiated to having the largest permeability values in this reservoir. The estimated average permeability of reservoir C stands at 1029.97mD, this signifying reservoir C to having excellent permeability values [8].

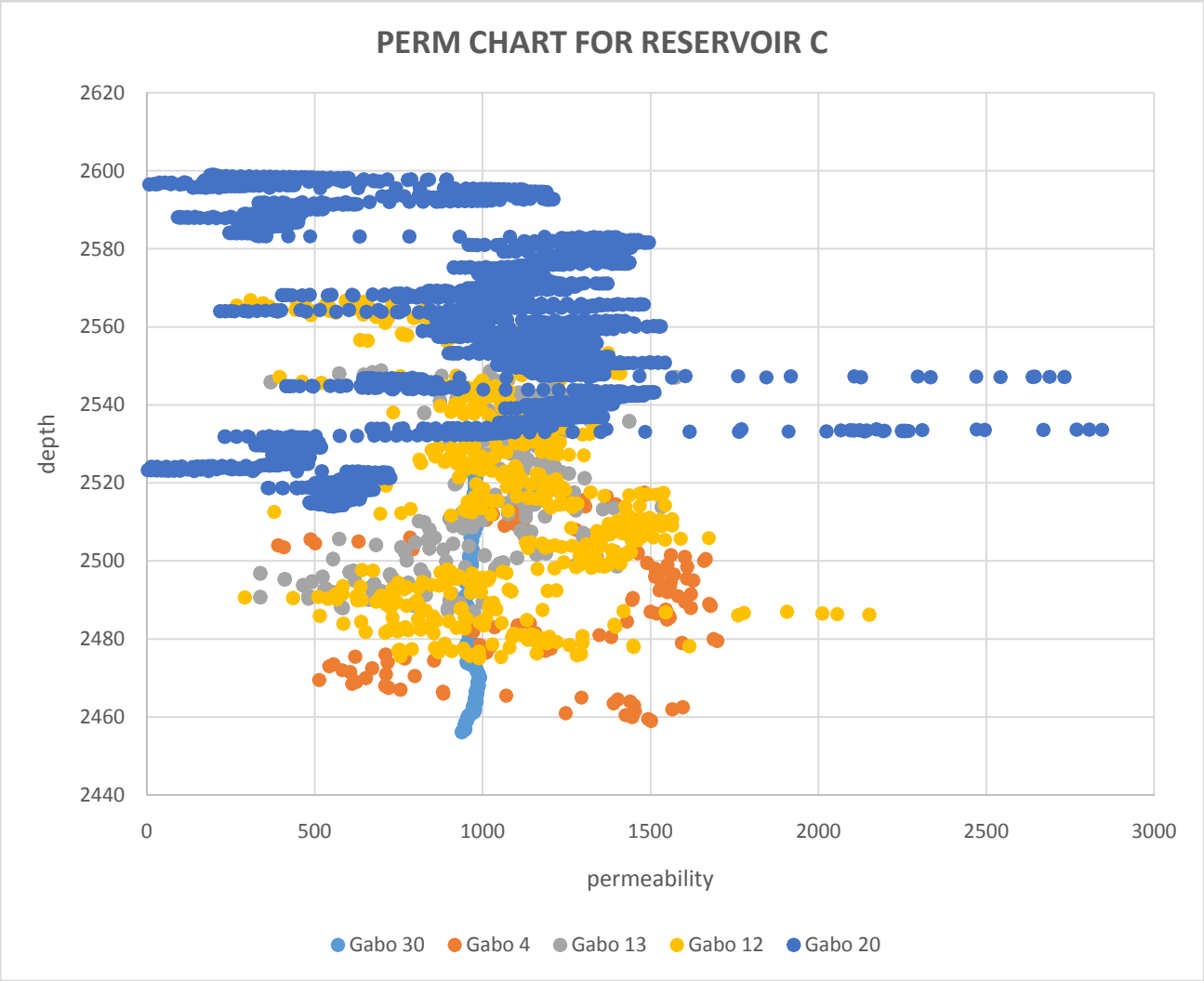

Fig 26. Permeability chart for reservoir C

C. Fluid saturation attribute

Crossplot of water saturation versus hydrocarbon saturation has been carried out in Figure 27. The result shows that, majority of the wells including Gabo 30, Gabo 4, Gabo 13 and Gabo 20 formed a linear regressive line, while Gabo 12 formed a concave curve below the linear values of the rest wells. The graphical representation of Gabo 12 depicts an equal proportion of water as well as hydrocarbon in the well. In addition, Gabo 20 has a high water ratio to hydrocarbon while Gabo 30, Gabo 4 and Gabo 13 show a higher proportion of hydrocarbon fractions compare to water.

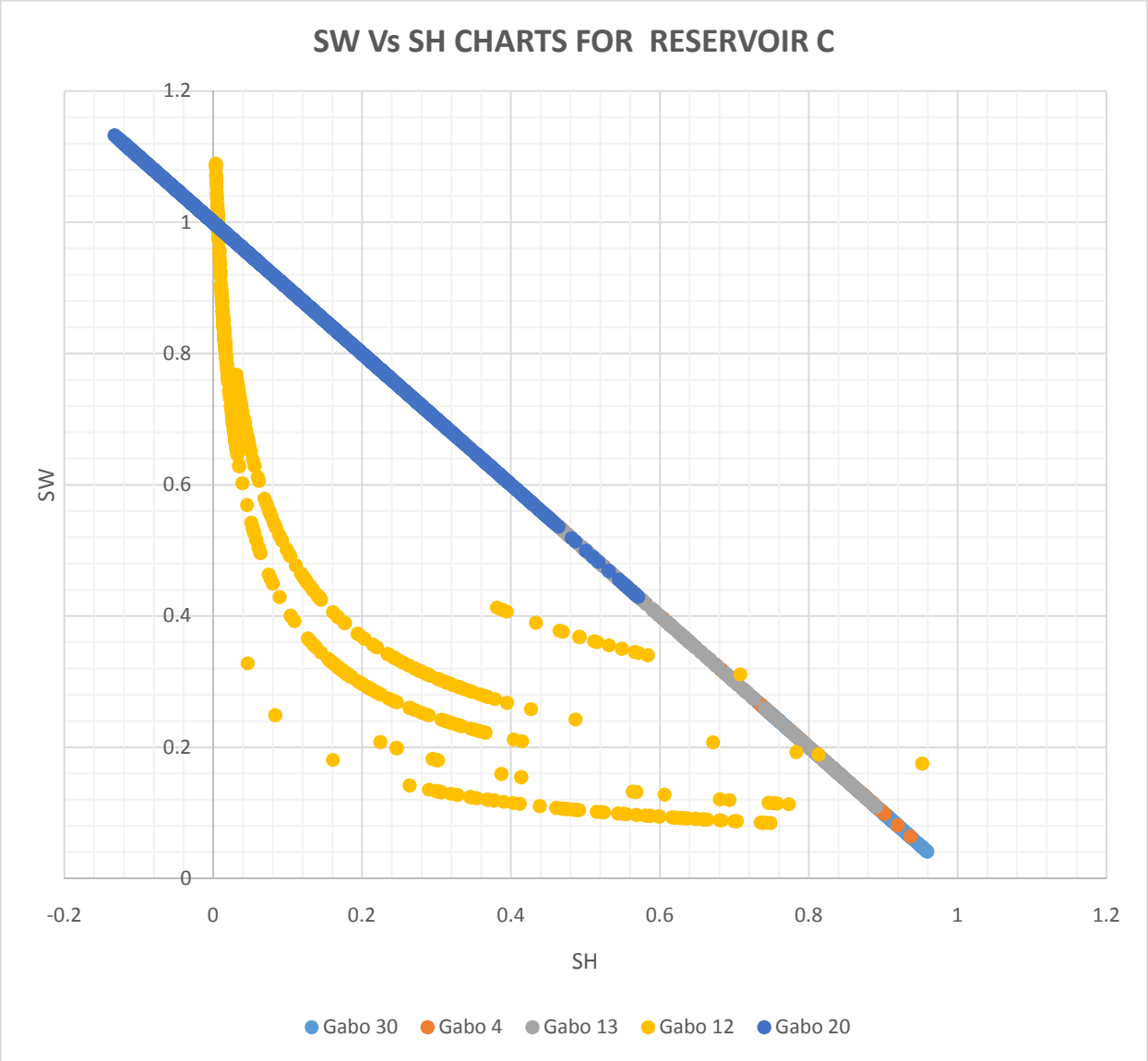

Fig 27. Crossplot of water saturation (Sw) vs hydrocarbon Saturation (Sh) chart for reservoir C

4. Petrophysical analysis of Reservoir D

Reservoir D has been picked from Top to Bottom across the wells having corresponding depth range of 2586.071ft – 2647.02ft for Tops as well as 2609ft – 26798.07 for reservoir Bottoms. The average thickness of this reservoir is 16.07ft, making it the smallest hydrocarbon reservoir in the field. Just like reservoirs A, Band C, all petrophysical attributes including volume of shale (vsh), total porosity (ϕt), effective porosity (ϕe), water saturation (Sw), hydrocarbon saturation (Sh) and permeability(mD) has all been analysed

across the wells (Gabo30, Gabo 4, Gabo 13, Gabo 12, and Gabo 20) in the reservoir.

A. Porosity Attributes

The result from porosity crossplot (water saturation vs hydrocarbon saturation) shows that porosity values has been arranged or propagated along a linear regressive line, delineating porosity discriminations across the wells. Magnitudes of porosity displacement across the wells has been negligible except for porosity values of Gabo 30 whose crossplot values looked so far apart from the rest of the wells (figure 28). The line regressive line formed from the crossplot of porosity parameters shows that porosity reduces with depth. Although Gabo 30 has been identified to having the best porosity properties, Gabo 20 appears to have the least porosity attributes across the wells.

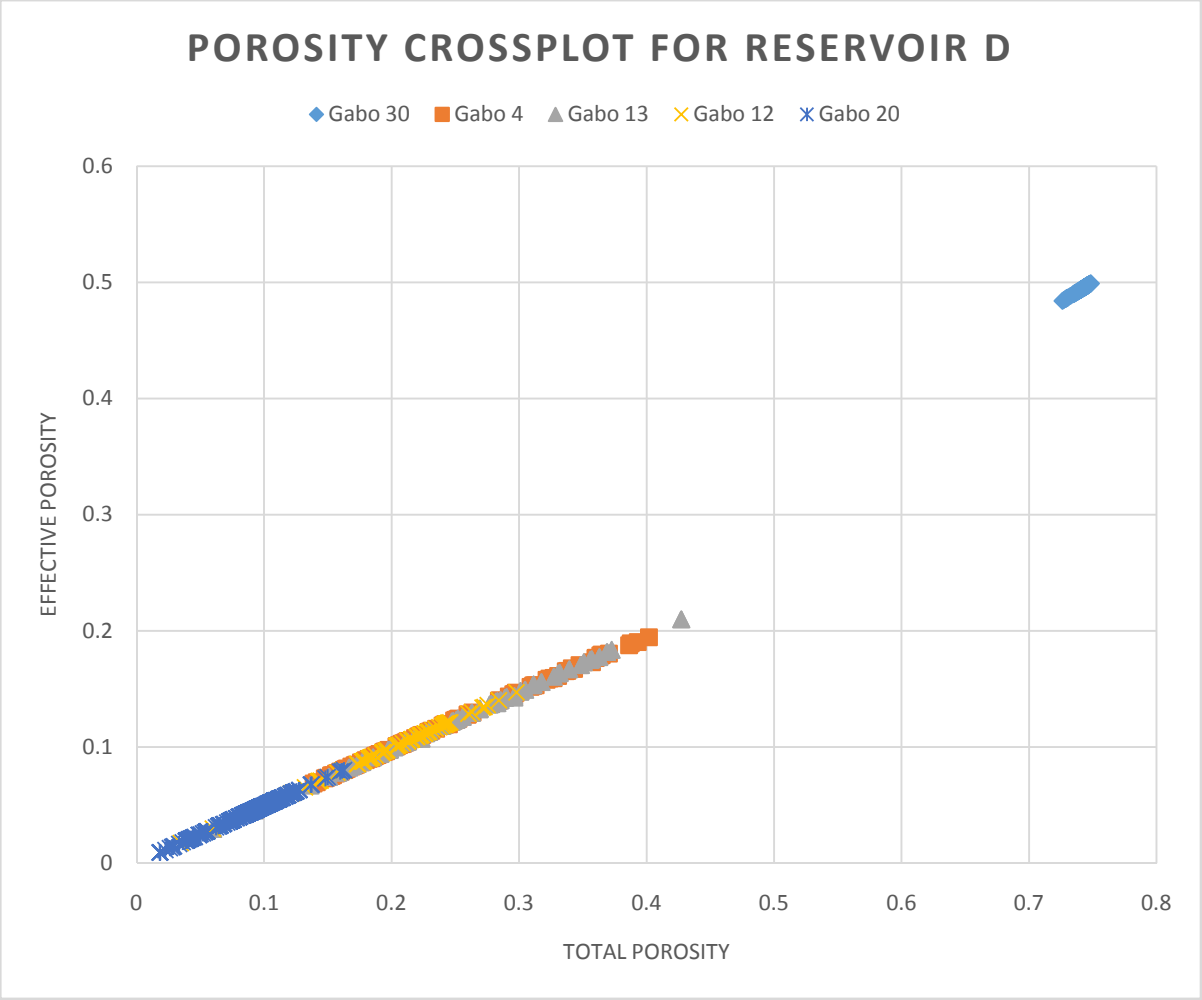

Fig 28. Porosity crossplot for reservoir D.

B. Permeability attributes

The permeability chart (Fig 29) of reservoir D shows that Gabo 13 and Gabo 4 have the highest permeability values and permeability increases with depth in these wells of interests. Permeability also increased with depth in Gabo 12 and Gabo 20, however Gabo 20 has been attributed to having the lowest porosity values from permeability delineations across the well in reservoir D. The average permeability value in reservoir D is 880.69mD, thus it has been deemed to have excellent permeability values according to Rider permeability classification.

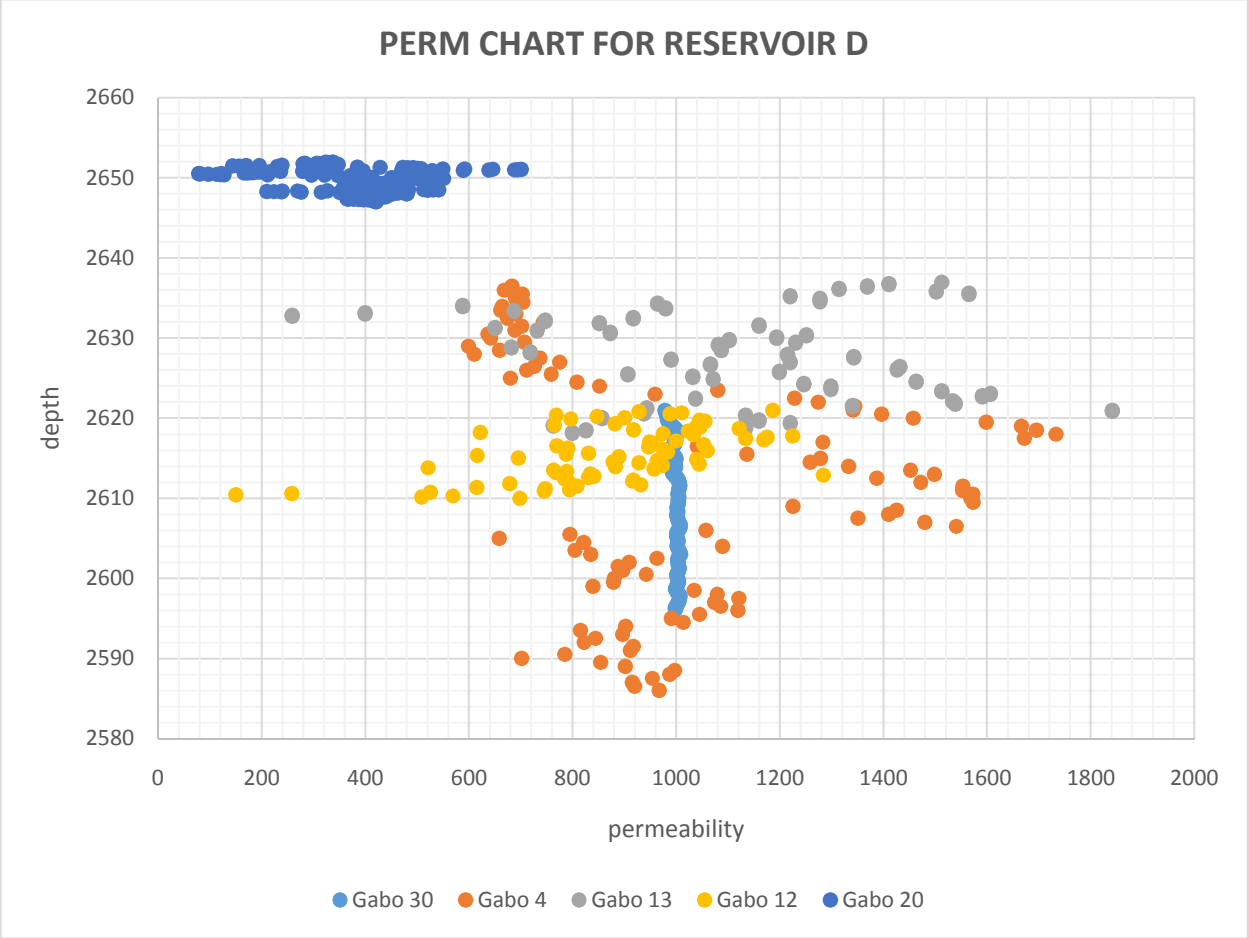

Fig 29. Permeability chart for reservoir D

C. Fluid saturation attributes

Figure 30 shows a crossplot of water saturation (Sw) and hydrocarbon (Sh). Furthermore, the delineation of this crossplot shows that a majority of fluid saturation values has been propagated along a linear regression line, with exceptions to crossplot values of Gabo 12. Fluid saturation attributes of Gabo 12 has been propagated along a concave curve just above the linear regression line. Due to the delineation of Gabo 12, it invariably suggests that the well has more water content than hydrocarbon saturating its void spaces. The linear delineation of Gabo 30, Gabo 4, Gabo 13 and Gabo 20 suggests that fluid saturation reduces significantly with depth in these wells of interest.

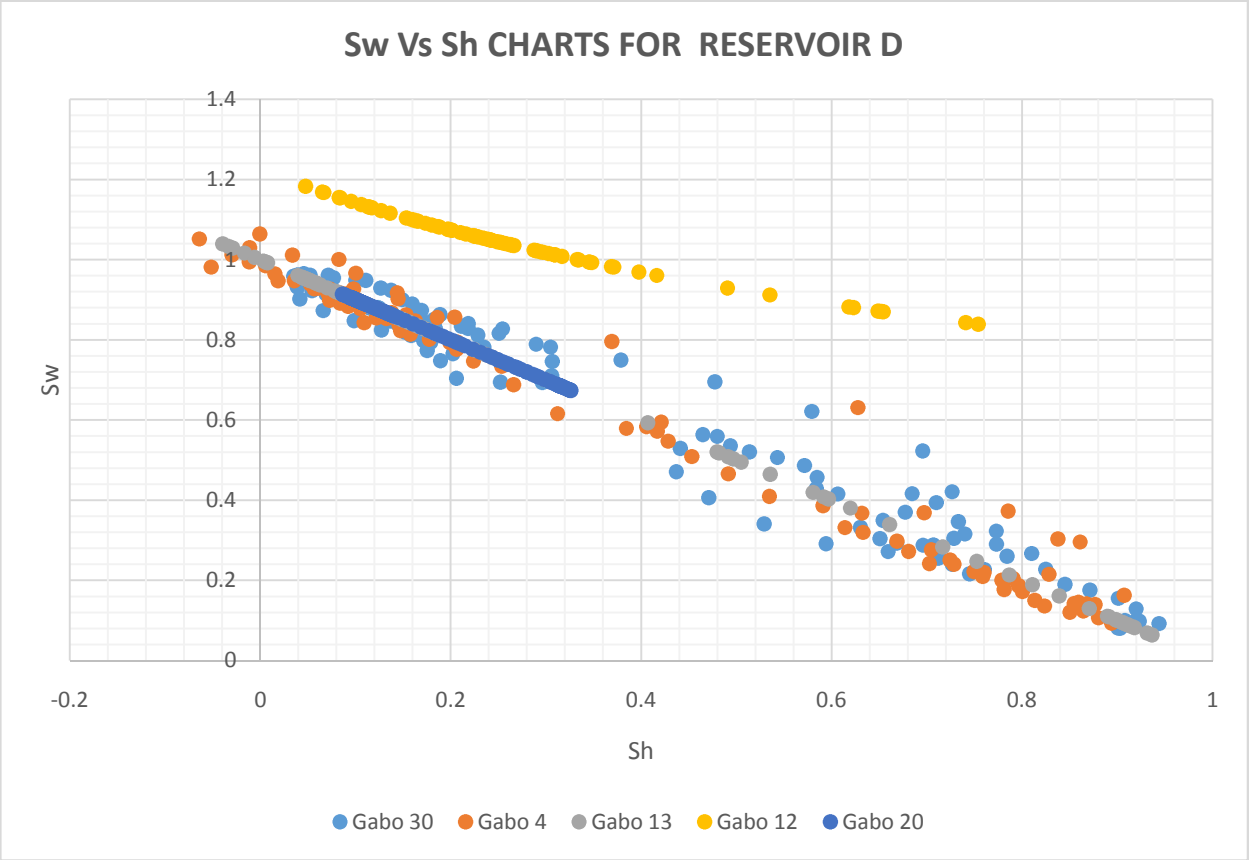

Fig 30. Crossplot of water saturation (Sw) vs hydrocarbon Saturation (Sh) chart for reservoir D

V. SUMMARY

Petrophysicalevaluation was consequently based on well logs, geological information of the study area and petrophysical calculations to determine the petrophysical parameters of the reservoirs in Gabo field.

The average thickness of reservoir A across the wells is 19.11ft. Effective porosity 11.80%, total porosity 23.96% and average Permeability 911.56mD. The reservoir shows good porosity as well as very good permeability. Water Saturation (Sw) and Hydrocarbon saturation (Sh) shows a fairly homogeneous composition.

The average thickness of reservoir B across the wells is 18.58ft. Effective porosity 9.89%, total porosity 20.04% and average Permeability 734.11mD. The reservoir shows very good permeability.

The average thickness of reservoir C across the wells is 71.92ft. Effective porosity 12.57%, total porosity 26.54 % and average Permeability 1029.97mD. The reservoir shows good to very good porosity and excellent permeability values. Equal proportion of water and hydrocarbon is observed in this reservoir.

The average thickness of reservoir D across the wells is 16.07ft. Average Permeability value 880.69mD. Gabo 30 having the best porosity, Gabo 20 appears to have the least porosity attributes across the well. The reservoir shows excellent permeability values.

VI. CONCLUSION

Four (4) reservoirs labelled A, B, C and D were identified and evaluated in the Gabo field. These reservoirs were interpreted as deposited in the shallow marine depositional environment (Coastal deltaic- outer Neritic).The reservoirs have good reservoir characteristics as shown by their petrophysical properties. Porosity estimates is highest observed in the channel and shoreface environment. Therefore, it is assumedthat this environment supports hydrocarbon accumulation.

ACKNOWLEDGEMENT

Thanks to the Department of Petroleum Resources(DPR) and Total Exploration and Production limited (Total E&P) for making the data available.

REFERENCES

[1] T. O. Adeoye, and P. Enikanselu, Reservoir mapping and volumetric analysis using Seismic and Well Data: *Ozean Journal of Applied Sciences, Vol. 2 Issue 4, 2009, 66-67,* 2009.

[2] Stat Oil Research Group, Geological Reservoir Characterization. Research and technology memoir 4, 2003.

[3] B. Vakareloy, Depositional bias in the subsurface: Symptoms and treatments. *Linkedin article publications,https://www.linkedin.com/pulse/depositional-bias-subsurface-symptoms-treatments-boyan-vakarelov/.* 2016.

[4]Schlumberger Limited, Cased Hole Log Interpretation: Principles/applications. Schlumberger wireline and testing, Houston Texas, 21-89, 1989.

[5]G. Asquith and B. Gibson. "Basic well log analysis for Geologists". *First edition American Association of Petroleum Geologist. Methods in Exploration Series, vol. 3, pp:216*, 1982.

[6] V. Larionov. Borehole Radiometry. Moscow, USSR, Nedra, 1969.

[7] O. O. Owolabi, T. F. Longjohn and J. A. Ajienka. "An empirical expression for permeability in unconsolidated sands of Eastern Niger Delta"; *Journal Petroleum geology. Issued. 17, vol. 1, 111-116*, 1994.

[8] M. H. Rider, The Geological Interpretation of Well Logs. *Whittles publishing, 2nd edition, Aberdeen,278*, 1996.

